MARIA S. MERIAN-Berichte

Molecular ecological chemistry in Arctic fjords
at different stages of deglaciation

Cruise No. MSM56

July 2 – July 25, 2016

Longyearbyen (Svalbard, Norway) – Reykjavík (Iceland)
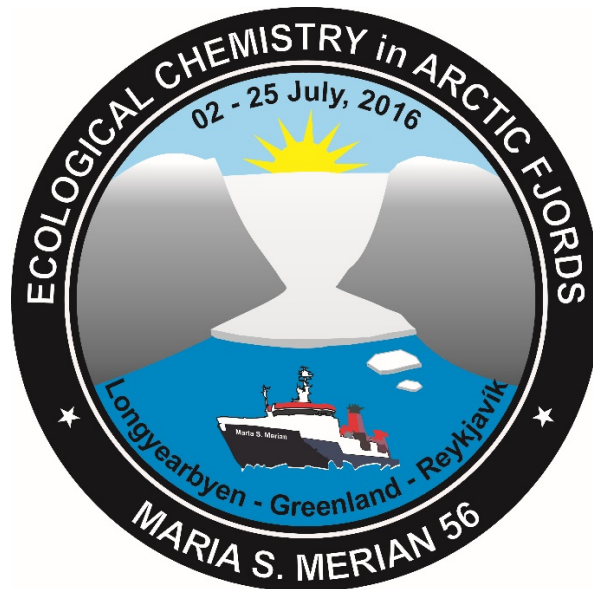
Koch B.P., John U., Amann R., Assmy P., Bach L., Burau C., Edvardsen B., Fernández-Méndez M., Friedrichs A., Geuer J., Hoppema M. (not on board), Huhn O. (not on board), Iversen M. (not on board), Konrad C., Kühne N., Lechtenfeld O.J., Mackensen A. (not on board), McCallister S.L., Nystedt E., Schmitt-Kopplin P., Schwalfenberg K., Seifert M., Stedmon C. (not on board), van de Waal D., van der Jagt H., Wohlrab S., Wulf J., Wünsch U., Zielinski O. (not on board)

The MARIA S. MERIAN-Berichte are published at irregular intervals. They are working papers for people who are occupied with the respective expedition and are intended as reports for the funding institutions. The opinions expressed in the MARIA S. MERIAN-Berichte are only those of the authors.

The MARIA S. MERIAN expeditions are funded by the *Deutsche Forschungsgemeinschaft (DFG)* and the *Bundesministerium für Bildung und Forschung (BMBF)*.

Author:

Prof. Dr. Boris Koch   Telefon:+49-471-4831 1346

Alfred-Wegener-Institut

Helmholtz Zentrum für Polar- und Meeresforschung

Am Handelshafen 12

27570 Bremerhaven

e-mail: Boris.Koch@awi.de

Table of Contents

1. Summary

The 22 participating scientists from Germany, Norway, the Netherlands, Denmark, Sweden, Finland and the United States covered scientific expertise in (micro-) biology, chemistry, and oceanography. Apart from aerosol and rainwater collection, which was applied to assess atmospheric deposition, sampling was restricted to the water column. Phyto and zooplankton were sampled by vertical net hauls using a plankton net, multinet and a pump system for the filtration of large water volumes to collect different size classes of phytoplankton, followed by DNA and RNA extraction. Phytoplankton was also characterized and quantified onboard by microscopy and flow cytometry. Primary productivity was assessed in incubations in the isotope container using radiocarbon labels. Clonal cultures were established to identify selected key species. Bacterial abundance, community composition and production were also determined onboard. Chemical sampling and analytical parameters, most of which taken from the CTD water sampler, will be measured back in the home labs. The final dataset will cover inorganic nutrients, oxygen concentration, dissolved inorganic carbon, total alkalinity, He/Ne ratios for the estimation of basal melt water, $\delta^{18}O$ for the contribution of meteoric water, particulate and dissolved organic carbon and nitrogen, optical properties (fluorescence), molecular characterization and radiocarbon age of organic matter.

A FerryBox system continuously recorded surface water information on turbidity, chlorophyll fluorescence, temperature, salinity, colored dissolved organic matter and salinity. At each station, salinity and temperature profiles were recorded by the CTD system and by profiler deployments, which also recorded the spectral light profile in the water column. The vertical material flux was investigated by the deployment of drifting sediment traps, a camera system and a marine snow catcher.

Zusammenfassung

Die 22 teilnehmenden Wissenschaftler aus Deutschland, Norwegen, den Niederlanden, Schweden, Finnland und den Vereinigten Staaten bearbeiteten die Themenfelder (Mikro-) Biologie, Chemie und Ozeanographie. Abgesehen von Aerosol- und Regenwasserbeprobungen, die für die Einschätzung der atmosphärischen Deposition erfolgten, beschränkte sich das Probennahmeprogramm auf die Wassersäule. Phyto- und Zooplankton wurden mit vertikalen Netzhols per Planktonnetz, Multinetz und Pumpsystem beprobt. Das Pumpsystem ermöglichte die Filtration großvolumiger Wasserproben und die Separation verschiedener Plankton-Größenklassen, deren DNS und RNS im Anschluss extrahiert wurden. Das Phytoplankton wurde an Bord zudem mit Hilfe von Mikroskopie und Durchfluss-Zytometrie charakterisiert und quantifiziert. Die Primärproduktion wurde durch Inkubationen mit Radiotracern im Isotopen-Container bestimmt. Klonale Kulturen wurden angelegt, um den phylogenetischen Status ausgewählter Schlüsselarten zu identifizieren. Bakterielle Zellzahlen, Artengemeinschaft und Produktion wurden ebenfalls an Bord bestimmt. Proben für chemisch/analytische Untersuchungen werden zum überwiegenden Teil aus den Wasserproben des Kranzwasserschöpfers nach Fahrtende in den Labors der Heimatinstitute bestimmt. Der finale Datensatz umspannt anorganische Nährstoffe, Sauerstoffkonzentration, gelösten anorganischen Kohlenstoff, Alkalinität, He/Ne-Verhältnisse zur Bestimmung des basalen Schmelzwasser, δ^{18}O zur Bestimmung des Beitrags des meteorischen Wassers, partikulären und gelösten organischen Kohlenstoff und Stickstoff, optische Eigenschaften (Fluoreszenz) und molekulare Charakterisierung und das Radiokarbon-Alter des organischen Materials.

Ein FerryBox-System zeichnete kontinuierlich Oberflächenwasserdaten zur Trübung, Chlorophyll-Fluoreszenz, Temperatur, Salzgehalt und den chromophoren Eigenschaften des gelösten organischen Materials auf. An jeder Station wurden Salzgehalts- und Temperaturprofile mit Hilfe der CTD und eines Profilers aufgenommen, der zudem Tiefenprofile des spektralen Lichts aufzeichnete. Der vertikale Materialfluss wurde mit Hilfe von driftenden Sedimentfallen, einem Kamerasystem und einem "marine snow catcher" bestimmt.

2. Participants

Name	Task	Institute
Koch, Boris	Marine Chemistry, Chief Scientist	AWI / UAB
Amann, Rudi	Prokaryotes; FISH	MPI
Bach, Lennart	Eukaryotes; Flow cytometry	GEOMAR
Burau, Claudia	Water chemistry; extraction	AWI
Edvardsen, Bente	Microalgal ecology; microscopy	UiO
Fernández-Méndez, Mar	Eukaryotes; incubations	NPI
Friedrichs, Anna	Oceanography: CTD, optical profiling	ICBM
Geuer, Jana	Water chemistry; trace elements	AWI
John, Uwe	Diversity; DNA/RNA extraction	AWI
Konrad, Christian	Grazing; sediment traps	MARUM
Kühne, Nancy	Eukaryotes; extraction	AWI
Lechtenfeld, Oliver	Water chemistry; radiocarbon	UFZ
McCallister, Leigh	Bacterial production; incubation	VCU
Nystedt, Elina	Eukaryotes; sampling	NPI
Schmitt-Kopplin, Philippe	Aerosol chemistry; sampling, extraction	HMGU
Schwalfenberg, Kai	Oceanography: CTD, optical profiling	ICBM
Seifert, Miriam	Water chemistry; pCO_2, oxygen	AWI
van de Waal, Dedmer	Eukaryotes; incubation experiments	NIOO
van der Jagt, Helga	Particle export; sediment traps	MARUM
Wohlrab, Sylke	Eukaryote diversity; extraction	AWI
Wulf, Jörg	Prokaryotes; FISH	MPI
Wünsch, Urban	Optical OM properties; fluorescence	DTU

AWI	Alfred-Wegener-Institut Helmholtz Zentrum für Polar- und Meeresforschung
DTU	Technical University of Denmark
GEOMAR	Helmholtz-Zentrum für Ozeanforschung
HMGU	Helmholtz Zentrum München, Deut. Forschungszentr. f. Gesundheit u. Umwelt
ICBM	Institut für Chemie und Biologie des Meeres der Universität Oldenburg
MARUM	Zentrum für Marine Umweltwissenschaften der Universität Bremen
MPI	Max-Planck-Institut für Marine Mikrobiologie
NIOO	Netherlands Institute of Ecology
NPI	Norwegian Polar Institute, Fram Centre
UAB	University of Applied Sciences Bremerhaven
UFZ	Helmholtz-Zentrum für Umweltforschung Leipzig
UiO	University of Oslo
VCU	Virginia Commonwealth University

3. Research Program

Global change causes fundamental environmental changes in the Arctic. Increasing temperatures result in melting of the Arctic ice sheet and glaciers and the increasing freshwater discharge inevitably leads to changes in Arctic fjord systems. Our study thus aimed at two major topics:

(i) Changes of the phyto- and bacterioplankton community along salinity gradients in Arctic fjords and (ii) the impact of such changes on biogeochemical fluxes and chemical modification of organic substrates and metabolites. Community composition is an important driver of particulate and dissolved matter partitioning and for the bioavailability of organic matter to grazers and microbes. Hence, carbon flux in the water column depends on primary production and respiration from both microbes and vertically migrating zooplankton flux feeders.

Our study aimed at comparing three Fjord systems (Kongsfjorden, Svalbard; Scoresby Sound, Greenland and Arnarfjörður, Iceland; Fig. 3.1), which differed in their extent of available scientific information, their size, geomorphology, glacier volume, extent of freshwater input, and their biogeochemical settings. Diurnal changes were studied during a time series station in the Scoresby Sound. From the results of our study, we expect new insights into how Arctic fjords respond to changes induced by climate warming.
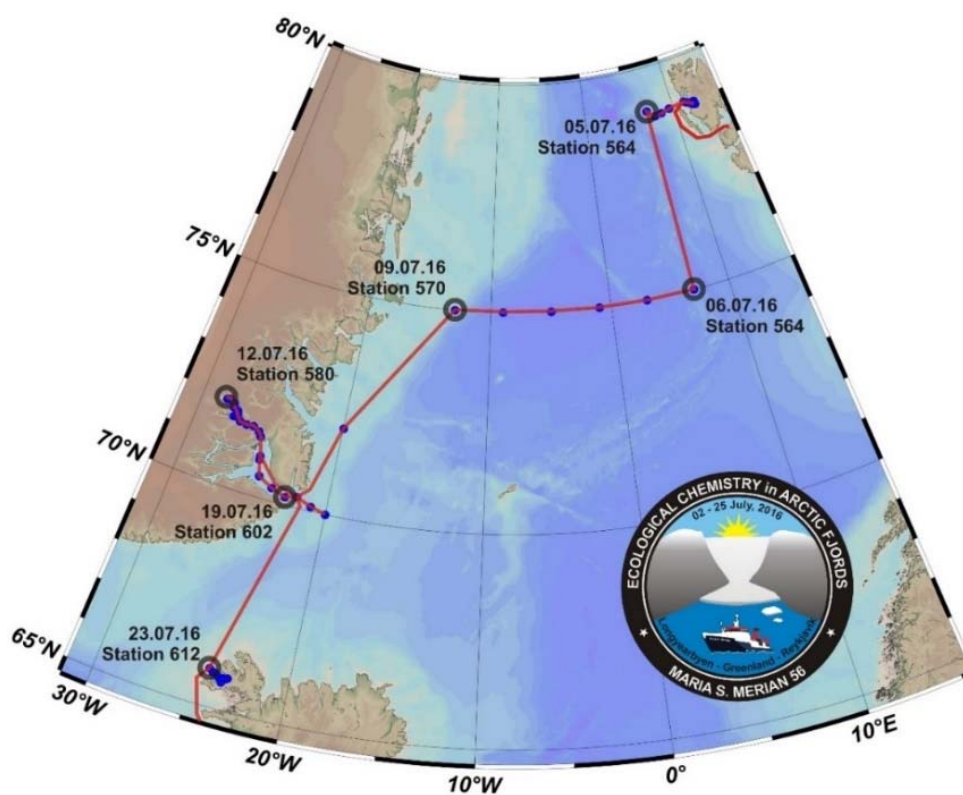
Fig. 3.1   Map of the sampling stations of the MSM56 research cruise conducted in the Arctic fjords Kongsfjorden (Svalbard), Scoresby Sound (Greenland) and Arnarfjörður (Iceland) and on a transect at 75°N in the East Greenland Sea.

4. Narrative of the Cruise

Maria S. Merian expedition MSM56 started early in the morning on July 2nd, slightly earlier than originally planned due to changes in the harbor schedule. During the transit from Longyearbyen to the first test station at the mouth of Kongsfjorden (

), the lab equipment and instruments were installed and a safety drill was carried out.

Generally, the sampling scheme differentiated between regular stations and "super-stations". On regular stations, the CTD water sampling rosette was deployed and samples for chemical and most biological parameters were taken. Super-stations additionally included large volume filtration and sediment trap deployments. In each fjord, glacier runoff and ice samples were collected using the ships zodiac. ADCP transects were carried out to assess water exchange.

Sampling locations in Kongsfjorden were aligned to the long-term monitoring program by the colleagues from the Norwegian Polar Institute (Fig. 4.1). After the first test station (551), the official sampling started at the toe of the Kongsbreen glacier at station 553 (equivalent to Norwegian station Kb7). Between, July 2nd and July 5th, we sampled a transect towards the mouth of the Kongsfjorden and further on to the Svalbard shelf. In sunny and calm weather conditions, we visited 13 stations, six of which were super-stations.
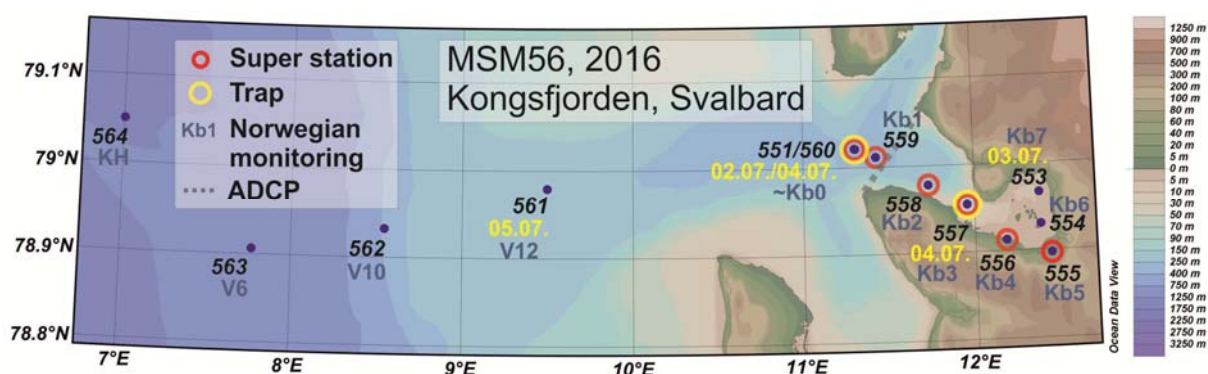
Fig. 4.1   Station map for Kongsfjorden and the Svalbard shelf. Yellow text assignments represent sampling date. Super-stations comprised all available sampling and analytical methods (red circles). Stations were aligned with the Norwegian monitoring program (blue abbreviations). One ADCP transect was performed at the exit of Kongsfjorden (dotted line).

In the evening of July 5th, we headed for the first station of a latitudinal transect on 75°N from Svalbard to Greenland. Six stations were sampled that complemented a Polarstern cruise (ARK 30-2, PS100), which took place almost simultaneously (July/August) and covered a transect along 79°N. After a stormy passage through the Greenland Sea and one coastal station on the Greenland shelf, we reached our main study area, the Scoresby Sound (Greenlandic: Kangertittivaq), on the evening of July 10th (Fig. 4.2). The ice conditions had improved substantially in the last few days so that we were able to instantaneously start our sampling in the mouth of the fjord. During the night, an ADCP transect was carried out to assess water exchange. In the morning of July 11th, we sampled two stations outside of the Scoresby Sound

and thereafter started the 350 km transit to the inner part of the Scoresby Sound (Nordvestfjord), where the Daugaard Jensen glacier terminates. On the way, we sampled four CTD stations (each of which was resampled on the return trip to the mouth of the fjord). In ice conditions with only little remaining sea ice and many icebergs, we were able to reach the glacier after 30 hours in the evening of July 12th.
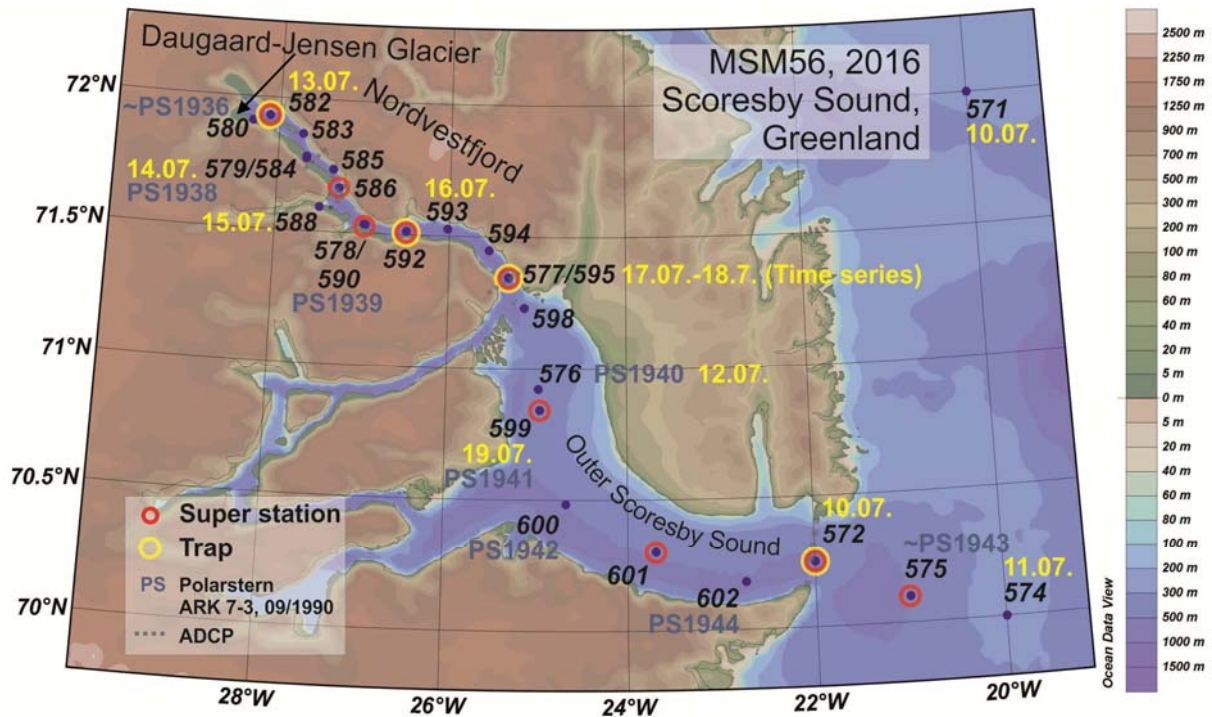
Fig. 4.2   Station map for Scoresby Sound and Greenland shelf. Yellow text assignments represent sampling date. Super-stations comprised all available sampling and analytical methods (red circles). Some stations were revisited stations of Polarstern cruise ARK7-3 (1990) (station number as blue abbreviations). Several ADCP transects were performed at the exit of Scoresby Sound and in Nordvestfjord (dotted lines).

The Daugaard Jensen Glacier drains approximately 4% of the Greenland Ice Sheet. Therefore, the density of icebergs was high so that the first station was still a few miles away from the glacier terminus. Several sampling locations were aligned with positions that were previously sampled by an expedition with research vessel Polarstern in September 1990 (cruise ARK VII-3). The first comparison with previous data showed identical salinity profiles but temperatures 0.5°C warmer in the deep fjord than 26 years ago. The sampling transect from the inner part of the fjord back to the mouth of Scoresby Sound covered 26 stations, eight of which were super-stations. During the transect on July 16th, we originally planned to start the time series station for the assessment of diurnal changes in the water column. However, we found only very little chlorophyll in the water and therefore postponed the time series. On July 17th, the algal production was still low and we decided to shorten the duration of the time series to 24 h and two tidal cycles at the outlet of the Nordvestfjord (station 595) followed by an echo-

sounder and ADCP survey to get a better picture of the bottom topography and water exchange. The echo-sounder transects showed that some areas at the entrance of the Nordvestfjord were much shallower than shown in the navigation maps. After our last station in Scoresby Sound (602), our transit to Iceland started half a day earlier than originally planned, in order to drop-off one member of the science team, who had to leave the ship for family reasons. In the morning of July 20th, the station work in the Arnarfjörður started (Fig. 4.3). The size of Arnarfjörður is comparable to the Kongsfjorden and represented an important ice-free reference. The stations were aligned with locations previously sampled during Maria S. Merian cruise MSM21 (August 2012). At partly cloudy weather conditions, we sampled nine stations, five of which were super-stations.
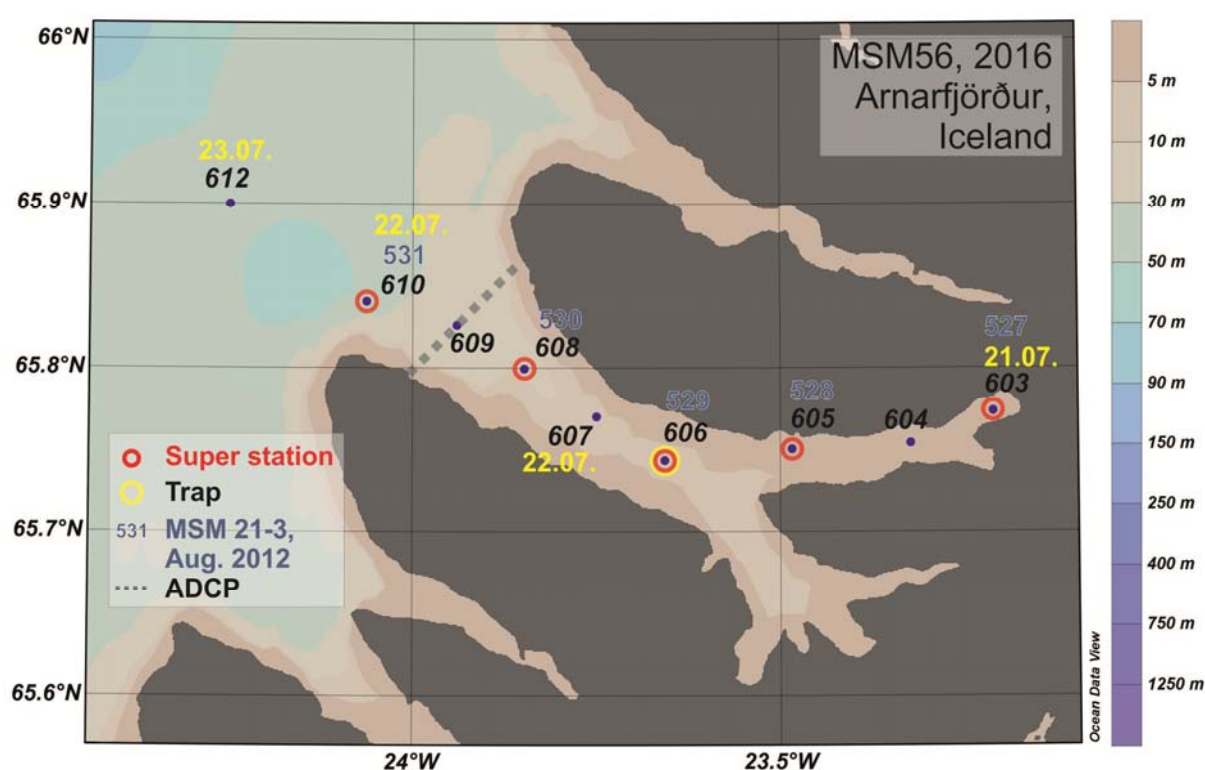
Fig. 4.3   Station map for Arnarfjörður. Yellow text assignments represent sampling date. Super-stations comprised all available sampling and analytical methods (red circles). Some stations were aligned with a previous with Maria S. Merian (MSM 21-3, blue numbers). One ADCP transect was performed at the exit of Arnarfjörður (dotted line).

The in-situ sampling was complemented with several on board experiments covering the photo and microbial degradation of organic matter in endmember samples such as Atlantic and Polar water, meltwater, and melted ice. Also, micro-zooplankton grazing and zooplankton feeding on fecal pellets were studied in additional experiments.

In total, we sampled 57 CTD stations, and six glacial runoffs and ice samples. We deployed 14 sediment traps, recorded 38 profiles with the particle camera, and performed 21 large volume filtrations.

5. Preliminary results

5.1   Bacterial community composition

(R. Amann, J. Wulf)

5.1.1   Onboard sampling

The quantitative phylogenetic analysis of bacterial community composition by ribosomal RNA-based methods is performed on non-fractionated material obtained from the CTD/Water-Rosette sampler. In addition, larger particulate material collected by the Marine Snow Catcher (MSC samples) and drifting sediment traps ("Arktische Drift-Falle"; ADF samples), both supplied by Helga van der Jagt, were fixed for later studies. In addition, we determined total cell counts for the incubation experiments of Oliver Lechtenfeld. All samples were fixed in 1% formaldehyde and subsequently collected on 0.2 μm filters for subsequent analyses for total cell counts (DAPI) and phylogenetic composition (CARD-FISH). 260 samples were retrieved from 40 stations.

5.1.2   Onboard data and first results

More than 300 filters were analyzed by DAPI staining for total cell count determination and catalyzed reporter deposition fluorescence in situ hybridization (CARD-FISH). Automated cell identification and counting was performed on ~ 20,000 fields of view, indicating that bacterial cell counts per mL were with $< 1*10^6$ lower in Scoresby Sound than in Svalbard and Iceland fjords where numbers were frequently in the range of 2-$3*10^6$ per mL. Phylogenetic staining with 16S rRNA-targeted oligonucleotide probes indicated a high prevalence of flavobacteria, in particular of members of the genus *Polaribacter*. Members of this clade are adapted to the degradation of algal polysaccharides. They could also be detected on the aggregate material collected in the marine snow catcher and sedimentation trap (example: Fig. 5.1).
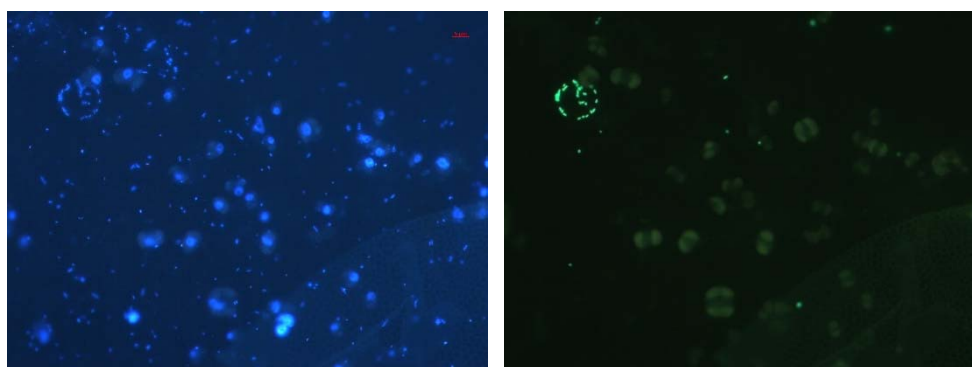
Fig. 5.1   Total DAPI cell counts (left, blue) and *Polaribacter* cells (right, green; identical FOV) identified by probe POL740 by CARD-FISH in Marine Snow Catcher sample #2 (MSC2).

5.1.3 Expected results

Based on the results of comparative 16S rRNA sequence analysis performed by the group of Uwe John, further CARD-FISH analysis will be done on the fixed filter samples. We will participate in the interpretation of the bacterial diversity data. These will guide the selection and de novo development of oligonucleotide probes for further quantifications of bacterial community composition by CARD-FISH. These data will ultimately be entered in multifactorial statistical analyses for elucidating correlations of bacterial community composition with biological (in particular phytoplankton) and environmental parameters.

5.2   Phytoplankton biomass, optical properties and primary productivity
   (M. Fernández-Méndez, E. Nystedt)

The aim was to quantify and characterize the phytoplankton community and its optical and physiological properties across salinity gradients to assess the impact of glacier melt water on primary productivity.

5.2.1   Onboard sampling

Phytoplankton samples were obtained on board from the CTD casts. In general, the upper 100 m of the water column were sampled at five or six different depths, except for primary productivity which was only determined in the chlorophyll maximum. A total of 46 stations were sampled for biomass (Chlorophyll *a;* Chl*a*), 42 for optical properties (particulate absorption and mycosporine-like amino acids; MAAs) and 32 for primary productivity (photosynthesis versus irradiance curves using the ^{14}C method (Fernandez-Mendez et al., 2015). In addition, four ^{13}C-^{15}N nitrate and ammonium addition experiments were performed (stations 557, 563, 595 and 606) to quantify the ratio between new and regenerated production in the Chl*a* max of each fjord. From each treatment, a 100 mL subsample concentrated to 10 mL was fixed with glutardialdehyde for future NanoSIMS analysis with the purpose of studying individual cells carbon and nitrate uptake.

5.2.2   Onboard data

Chl*a* was measured on board with a Turner bench fluorometer after overnight extraction with methanol. Net primary production was measured on board using the scintillation counter in the radioisotope container. Counts per minute were converted to carbon uptake assuming an average Arctic seawater dissolved inorganic carbon (DIC) concentration. The optical properties (particulate absorption and MAAs) will be measured back at the home laboratories (particulate absorption at the Norwegian Polar Institute and MAAs at the University of Manitoba, Canada).

5.2.3   First results

Preliminary results suggest that all fjords were in a post bloom or late bloom situation, although this needs to be confirmed with the nutrient data. The integrated Chl*a* for the upper 50 m ranged between 27 and 56 mg Chl*a* m^{-2} in Kongsfjorden, with the highest Chl*a* values towards the mouth of the fjord and a significant deep Chl*a* max at 65 m depth (3.5 µg Chl*a* L^{-1}) that turned out to be actively photosynthesizing when exposed to light (Fig. 5.2). The four stations outside Kongsfjorden in the "AWI Hausgarten" area had Chl*a* standing stocks of 109-159 mg Chl*a* m^{-2}. During the Fram Strait transect at 75°N we encountered a deep Chl*a* max around 30 m with high Chl*a* values (up to 12 µg L^{-1}). In Scoresby Sound, Chl*a* concentrations were very low at the surface and generally low across the entire Nordvestfjord. In this area, the Chl*a* max was at 20 m depth and never exceeded 1.5 µg Chl*a* L^{-1}. On the contrary, Arnarfjörður

in Iceland showed higher Chl*a* (up to 8.7 μg Chl*a* L^{-1}) at 15 m. The phototrophic standing stock in Scoresby Sound was 21-159 mg Chl*a* m^{-2} while in Arnarfjörður it was 44-240 mg Chl*a* m^{-2}.

In terms of primary productivity, it seems that all communities in Kongsfjorden were photo-inhibited at light intensities >400 μmol photons m^{-2} s^{-1}. The Chl*a* normalized carbon uptake rates in Kongsfjorden were all lower than 1 μg C h^{-1}. The depth integrated primary production in Kongsfjorden ranged between 100 and 700 mg C m^{-2} d^{-1}, which is in the range of previously reported values for this fjord in summer. These are preliminary results based on calculations using an assumed DIC concentration and Chl*a* depth profiles interpolated from the 2-3 measurements performed until 30 m depth. The other fjords will be processes as soon as the DIC and fluorometer calibrated Chl*a* are available.
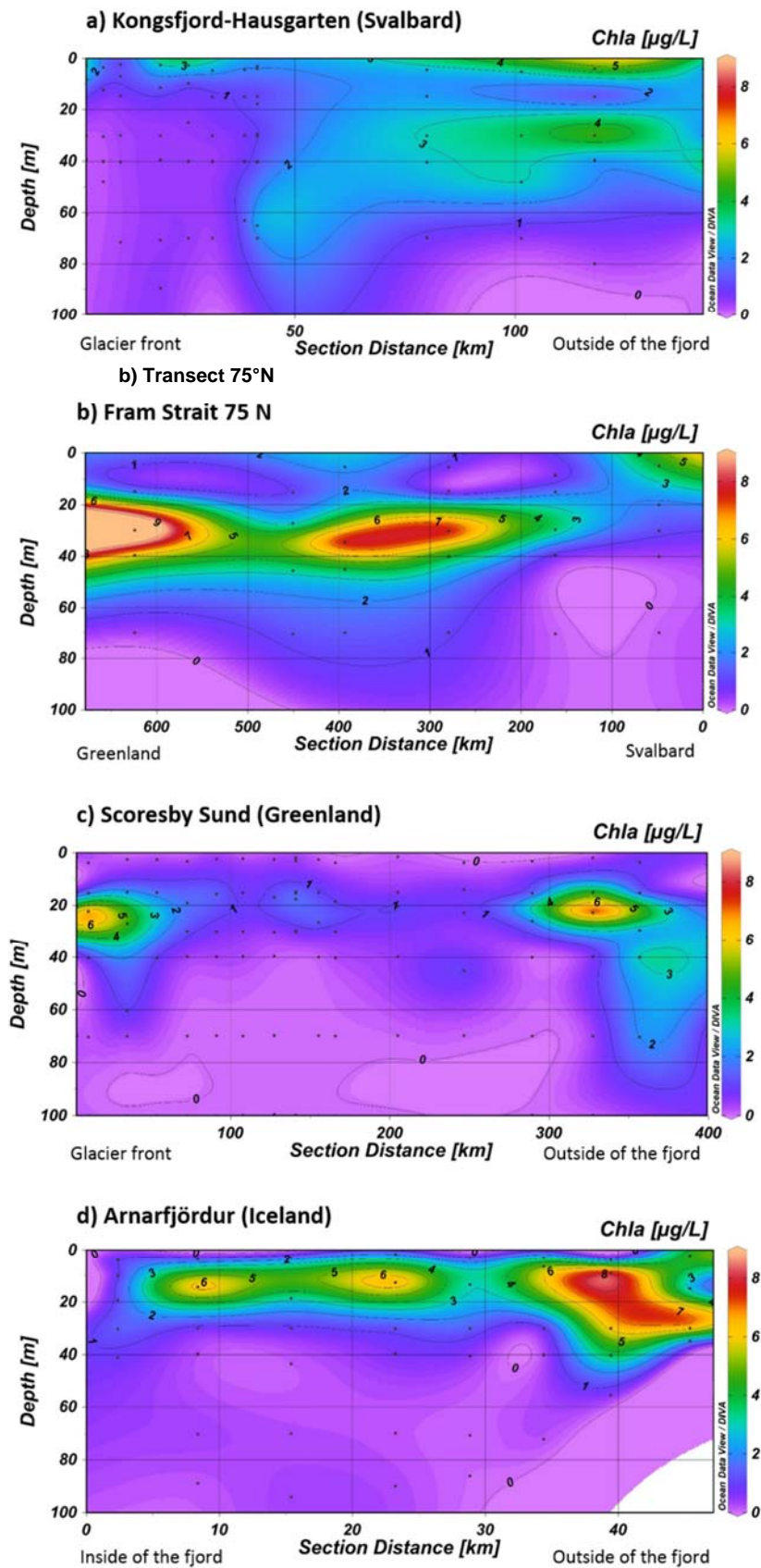
Fig. 5.2   Chla profiles of (a) Kongsfjorden (Svalbard), (b) Fram Strait transect, (c) Scoresby Sound (Greenland) and (d) Arnarfjörður (Iceland).

5.2.4   Expected results

Final estimates of in situ net primary productivity in the water column will be calculated using the fitted photosynthesis-irradiance (PI) curves according to the equation of Platt et al., (1982) and the light intensities measured with the profiler. The integrated carbon uptake rates for the water column will be assessed together with the carbon export, the bacterial respiration, and the zooplankton carbon demand, as well as with the particulate and dissolved organic carbon (POC, DOC) pools to get an idea of the carbon budget of the different fjords. The new versus regenerated production experiments will be analyzed in collaboration with the University Laval (Canada) and the NanoSIMS samples in collaboration with Stanford University. Particulate absorption will be measured back at the Norwegian Polar Institute and MAAs will be measured at the University of Manitoba (Canada). The optical properties of phytoplankton in the fjords will be interpreted together with CDOM measurements (U. Wünsch).

5.3   Physical oceanography and bio-optical properties in arctic fjords
   (A. Friedrichs, K. Schwalfenberg, O. Zielinski (not on board))

We aimed at an assessment of physical and bio-optical properties within arctic fjords based on temperature, salinity, photosynthetically available radiation (PAR), spectral downwelling irradiance and upwelling radiance, and fluorescence of Chl*a*.

5.3.1   Onboard data

Physical and bio-optical parameters were recorded on board. At each station, the downcast profile of temperature, conductivity, PAR, dissolved oxygen, turbidity and Chl*a* fluorescence was recorded with the CTD. Additional continuous measurements were conducted with a flow-through FerryBox system attached to the ship's seawater-pumping system. The system recorded temperature, conductivity (salinity), CDOM concentration, Chl*a* concentration, and turbidity.

The quasi-free falling spectral light profiling system, equipped with irradiance and radiance sensors, a fluorometer, backscatter sensor and a CTD, was deployed on most stations. The recorded light profile were conducted to a depth at which 1% light availability was reached and comprised downwelling irradiance and upwelling radiance from 380 nm up to 712 nm. PAR profiles were computed from the downwelling irradiance. A reference radiometer measured downwelling surface irradiance to represent 100% intensity of light availability above surface.

At selected stations, water samples were taken for calibration of the salinity data. Water turbidity was assessed via the deployment of a Secchi-Disk and water colour was measured via the Forel-Ule-index at each station. Current data was recorded using an ocean surveyor Acoustic Doppler current profiler (ADCP) on two different frequencies. One ADCP measured with 38 kHz to cover the water column up to 1500 m at its maximum and the second ADCP measured with 75 kHz with a finer resolution down to 800 m water depth.

5.3.2   First results

The salinity of discrete water samples for calibration was determined by an OPS003 salinometer, which was calibrated prior to each measurement. For the re-calibration of the CTD conductivity sensor data, a linear regression was applied between salinity of water samples (n=20) and the salinity value of the respective CTD depth (Fig. 5.3) and outliers were eliminated (Fig. 5.3, red circle). The second salinity sensor was also corrected by a linear regression (m = 1.0215, y(0) = -0.754), prior to data upload in PANGAEA. The measurements of the two available temperature sensors matched very well with an averaged ΔT of 0.0008 K. The usage of sensor one for temperature and salinity is recommended for calculations and further analysis.
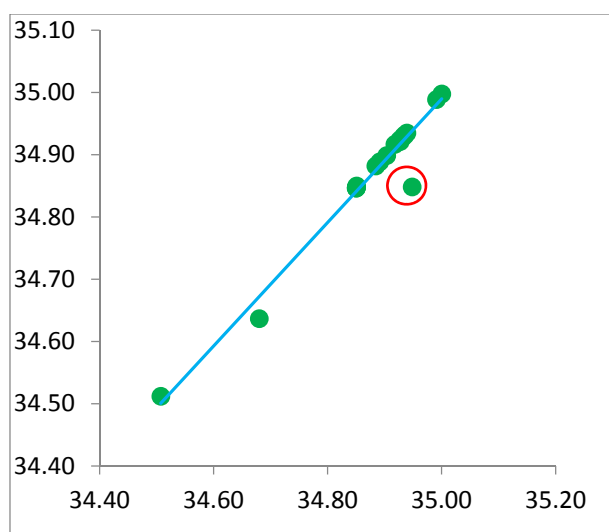
Fig. 5.3   Salinity sensor one correction is based on discrete samples (n=20) with following equation y=1.0215*x-0.754 achieved by linear regression (R² = 0.99; red marked outlier removed).

Visiting three fundamentally different fjord systems, Kongsfjorden, Scoresby Sound and Arnarfjörður allowed a detailed comparison of their physical oceanography. Melt water influence from glaciers, which was absent in Arnarfjörður, stood out in salinity data of Scoresby Sound and Kongsfjorden. As a consequence of the glacial influence, the milky surface layer reduced transparency and light availability in the upper meters of the water column. Details of oceanographic data for each of the three fjord systems and the transect at 75 °N crossing from East to West the Greenland basin are represented in the next chapter.

Kongsfjorden
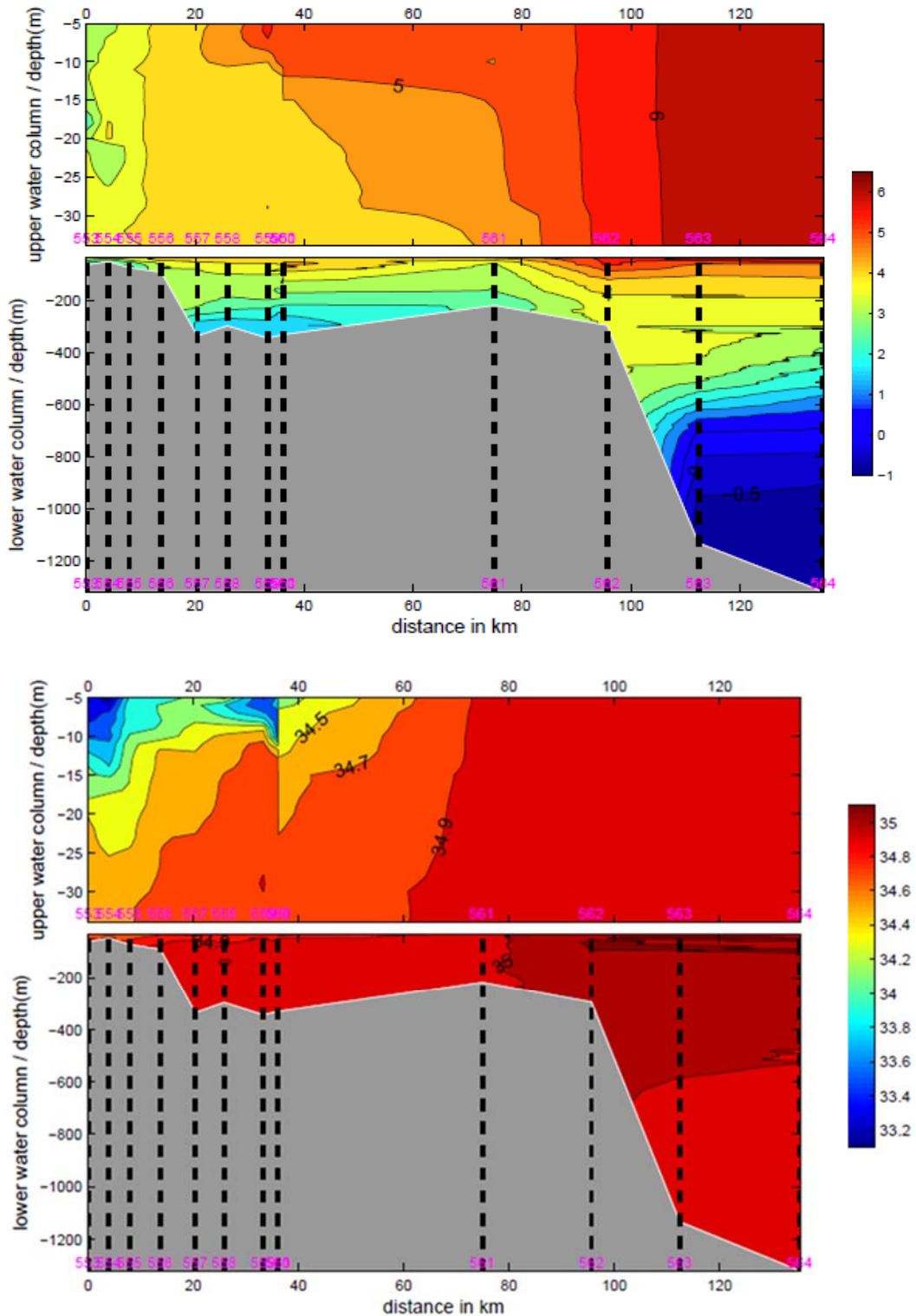
Fig. 5.4   Top: Temperature [°C] and salinity (bottom) of the Kongsfjorden section, separated in upper (< 40 m) and lower water column. Stations marked with black dashed lines and station numbers. Stations are ordered from the tip to the mouth of the fjord-system.

In Kongsfjorden, a thin, fresh (salinity < 33.2) and warm surface layer was located above a stable and salty (>34.4) layer that showed decreasing temperatures from 7°C near the surface and 1°C at the bottom. The surface layer (0 – 35 m) showed a spatial gradient with increasing salinity from areas influenced by glacier melt water (< 33.2) towards the mouth of the fjord (~34.9). The deep offshore stations 561 – 564 (Fig. 5.4) showed a strong vertical gradient in temperature (Fig. 5.4, top) from 6°C in the surface to – 1°C while salinity (34.9) showed no changes (Fig. 5.4, bottom). Surface water (up to 200 m water depth) was dominated by North Atlantic Water (NAW) while below cooler and fresher water was observed. The glacial melt water, characterized by low salinity and high turbidity, was also recognized by the quasi free-falling spectral sensor that measured bio-optical parameters such as Chl*a* fluorescence, turbidity, backscattering and irradiance and radiance.
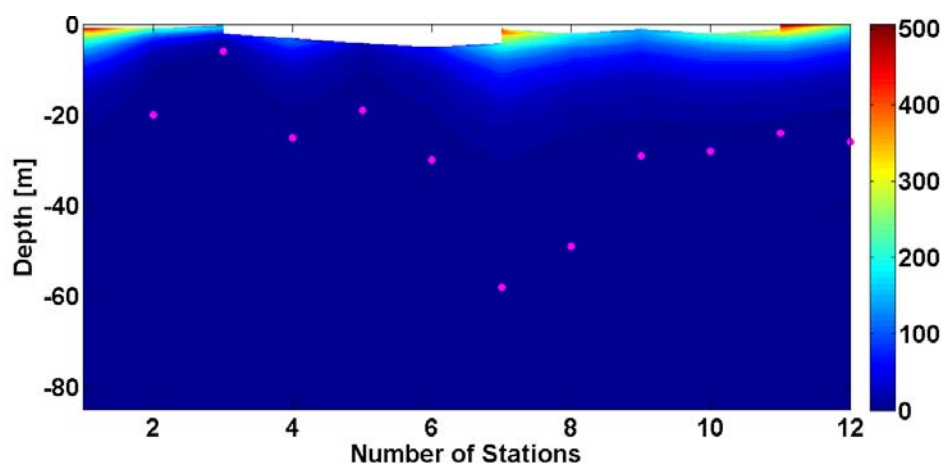
Fig. 5.5   Preliminary results of uncalibrated PAR [μmol/m²s] data down to the 1% light depth (dots).

First results for photosynthetically available radiation (PAR) showed an expected decline of PAR with depth (Fig. 5.5). The 1% depth of PAR was reached at different depths, which defined the photic zone for each station. Since the instrument only provided reliable data within a range of ±5 degree of tilt angle, the surface values were removed due to a larger tilt. In general, the light penetration depth was especially shallow in regions where a milky surface layer due to glacial melt water input was observed (station 3, Fig. 5.5). The other stations showed typical light penetration depths of 20-30 m at stations 9 to 12. Penetration depths of >50 m need to be verified by further analysis of bio-optical data.

Transect at 75 °N
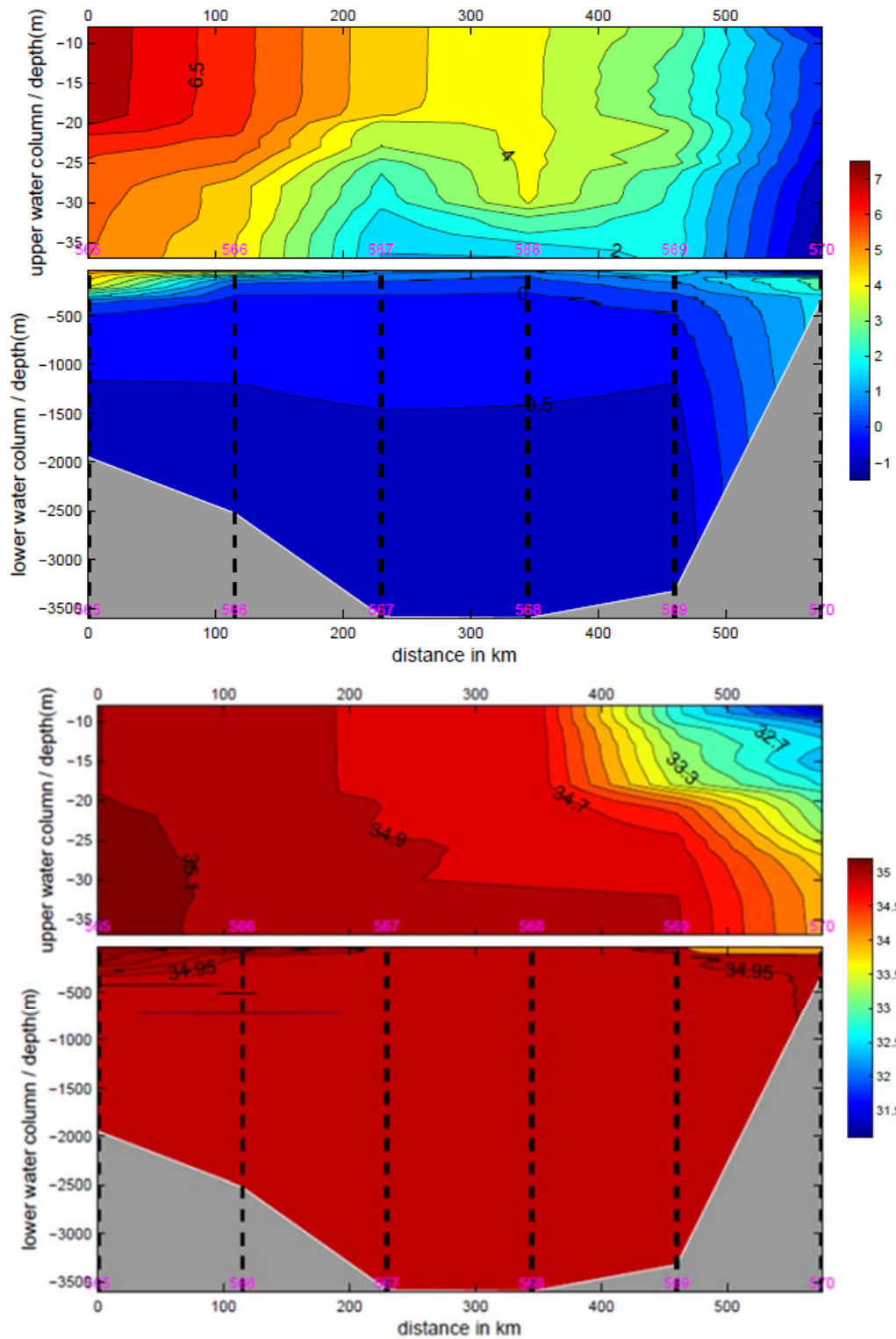
Fig. 5.6   Top: Temperature [°C] and salinity (bottom) section of Transect at 75 °N separated in upper (< 40 m) and lower water column. Stations marked with black dashed lines and magenta stations numbers. Stations ordered from East (left) – West (right).

The transect for the passage through the Greenland basin at 75°N showed constant temperature (Fig. 5.6, top) and salinity (Fig. 5.6, bottom) in the subsurface and a distinct horizontal gradient from high temperatures (~7°C) in the East to low temperature of ~0°C in the West near the Greenland Coast. The horizontal gradient in the surface resulted from two dominant surface water masses: the Atlantic Water in the East and Arctic Water in the West transported by the West Spitsbergen Current and East Greenland Current, respectively.
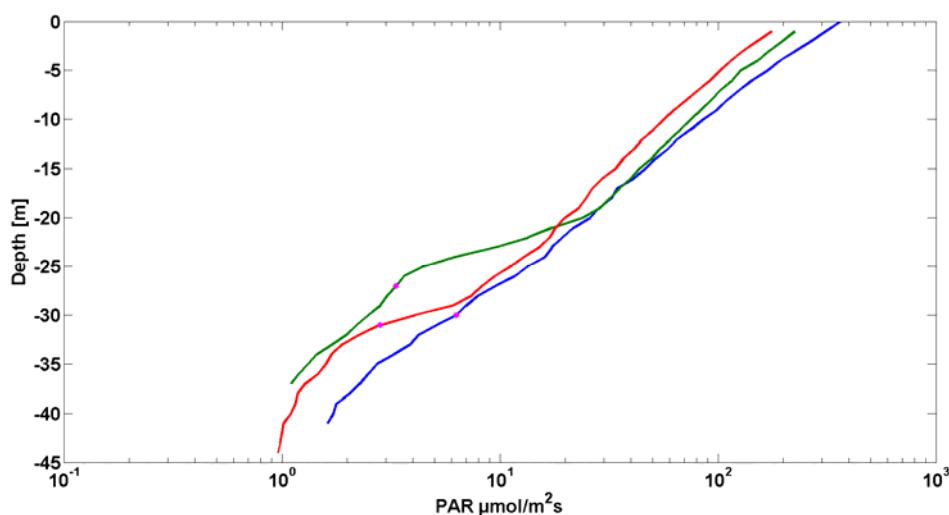
Fig. 5.7   Logarithmic PAR profiles for three stations on the transect along 75°N.
Dots represent 1% PAR depth.

Due to the weather conditions, only three stations allowed the deployment of the light profiler (Fig. 5.7), resulting in 1% PAR depth between 30 m and 40 m, comparable to the penetration depth observed at stations 9 to 12 in the Kongsfjorden section (Fig. 5.5).

Scoresby Sound
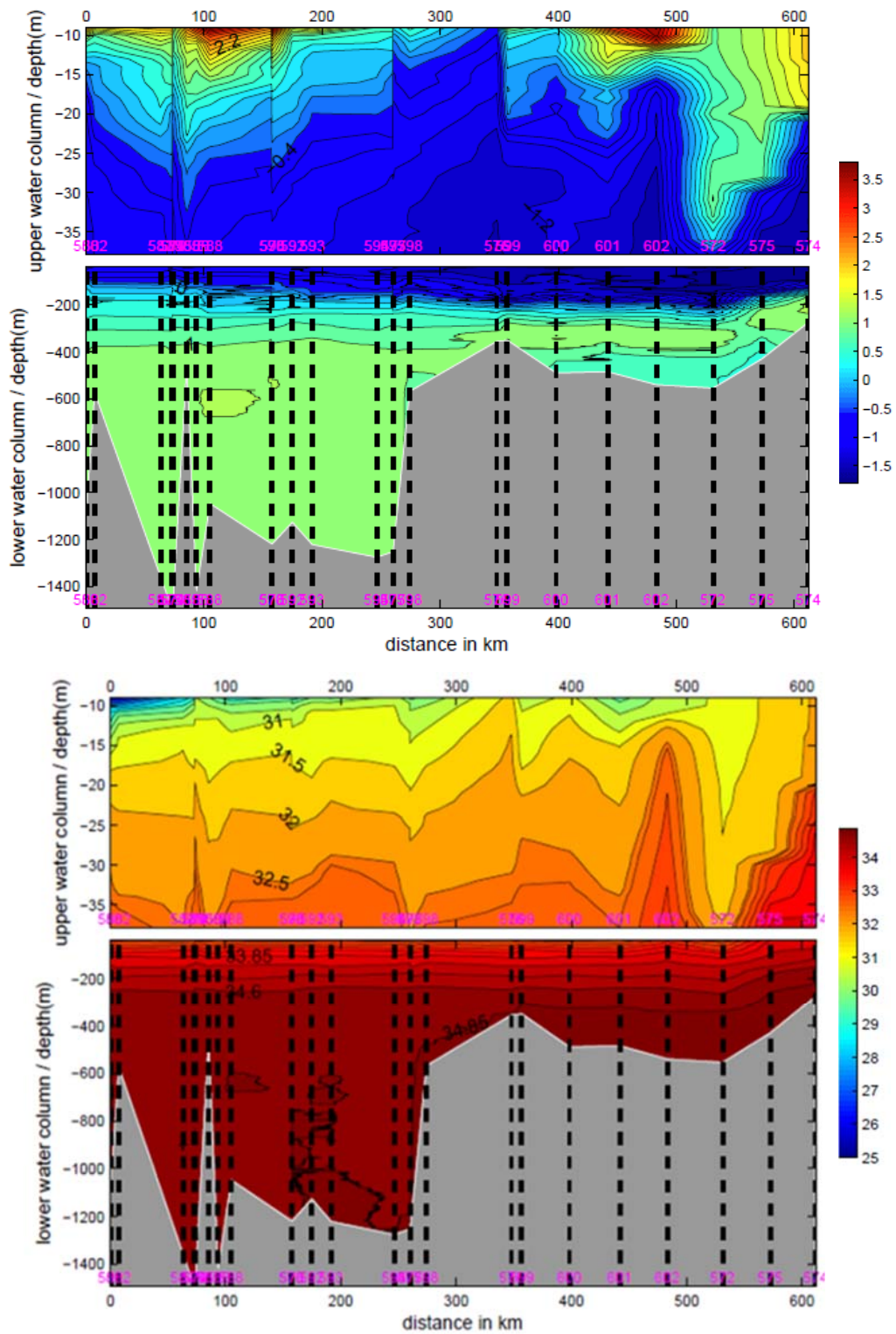
Fig. 5.8   Top: Temperature [°C] and salinity (bottom) at Scoresby Sound separated in upper (< 40 m) and lower water column. Stations marked with black dashed lines and station numbers. Stations are ordered from tip to mouth.
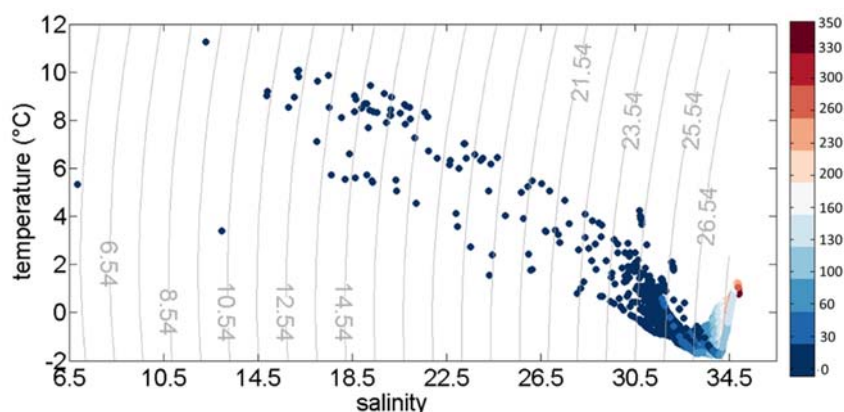
Fig. 5.9   Temperature [°C] – Salinity – diagram including density lines (gray) at Scoresby Sound.

Temperature profiles in Scoresby Sound showed a cold intermediate layer (< -1°C) and a warmer (up to 3°C) surface and bottom layer (up to 0.5°C). Below a thin (~5 m) surface layer influenced by freshwater (salinity > 20), a water body with higher salinity was recorded (Fig. 5.8). The T-S-diagram showed a shift of water masses from the inner to the outer part of Scoresby Sound with low-salinity in the surface of several stations (Fig. 5.9). Surface water varied from 6.5 to 30.5 in salinity and from -2 to 11°C temperature (Fig. 5.10). The layer below had a constant salinity around 34.5 and a temperature of 0°C +/- 2°C. The fresh surface layer was also recorded by flow-through data (Fig. 5.10, bottom), especially in the glacier-dominated Northwest-Fjord. In the Outer Scoresby Sound salinity was different between the north (first day of sampling) and the south (last sampling) (Fig. 5.10, bottom) which is likely a result of tidal and current water movement. In the southern part of the mouth of Scoresby Sound, water with lower salinity moved from west to the open ocean, whereas in the North saltier water was transported into the inner part of the fjord.
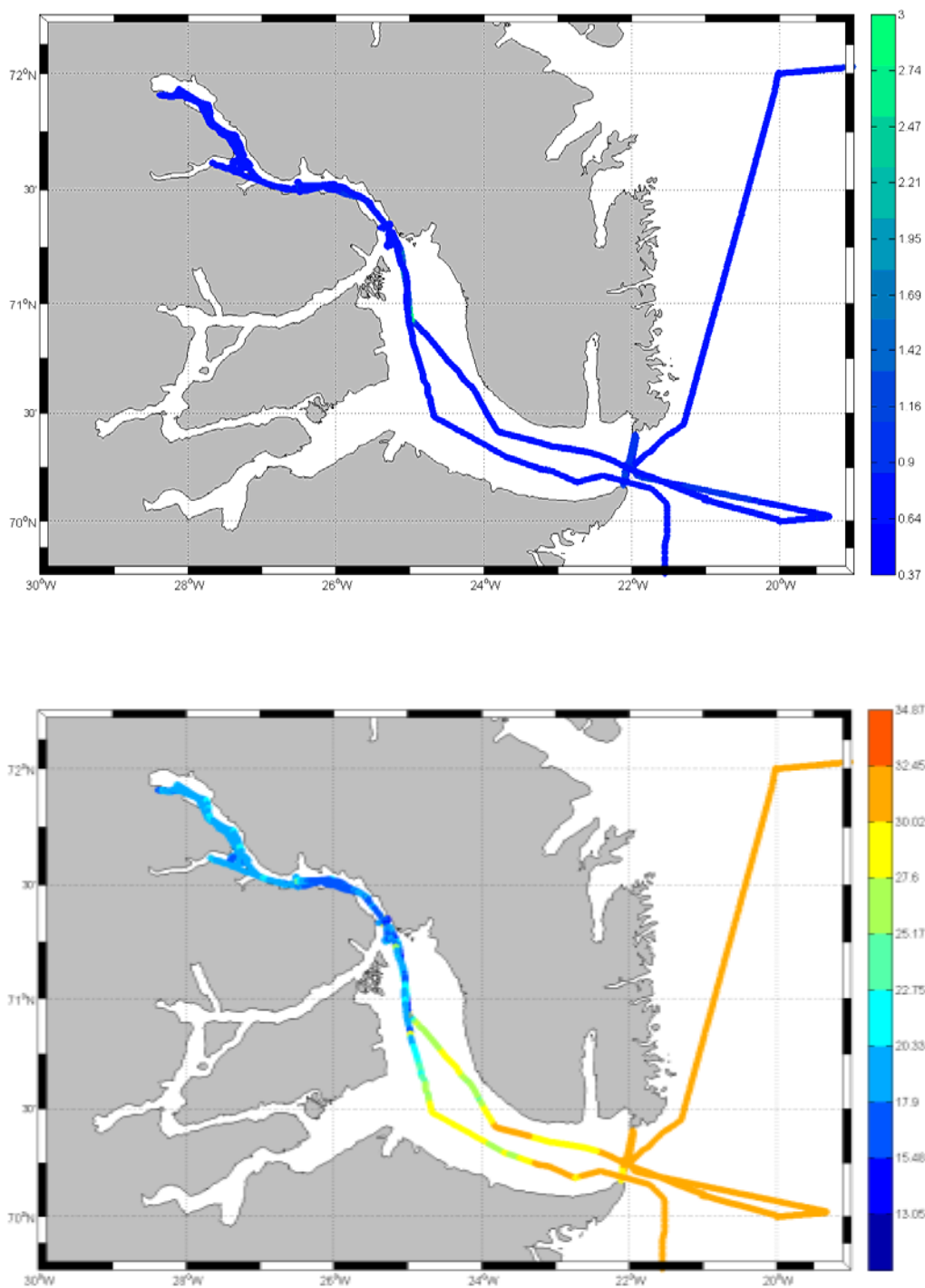
Fig. 5.10   Surface values delivered by the flow-through system FerryBox for Chla in mg/m³ (top) and salinity (bottom) for Scoresby Sound.

Chl*a* concentrations in the surface layer were generally below 2 mg/m³ (Fig. 5.10, top). Weather conditions in Scoresby Sound were sunny and calm, which allowed several deployments of the quasi-free falling spectral sensor. Compared to the other fjord systems, PAR was intense in the surface water of Scoresby Sound (up to 800 µmol/m²s; Fig. 5.11). Even when a milky surface was observed, the light penetrated relatively deep into the water column resulting in deep 1% PAR depths.
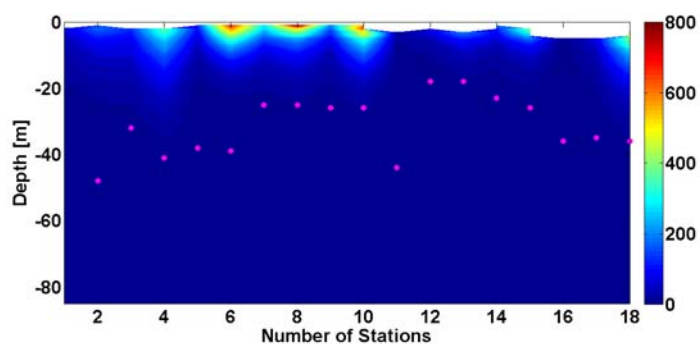
Fig. 5.11   Scoresby Sound (tip to mouth); Photosynthetically available radiation (PAR [µmol/m²s]) including 1% depth (magenta points) by free-falling light profiler.

Arnarfjörður
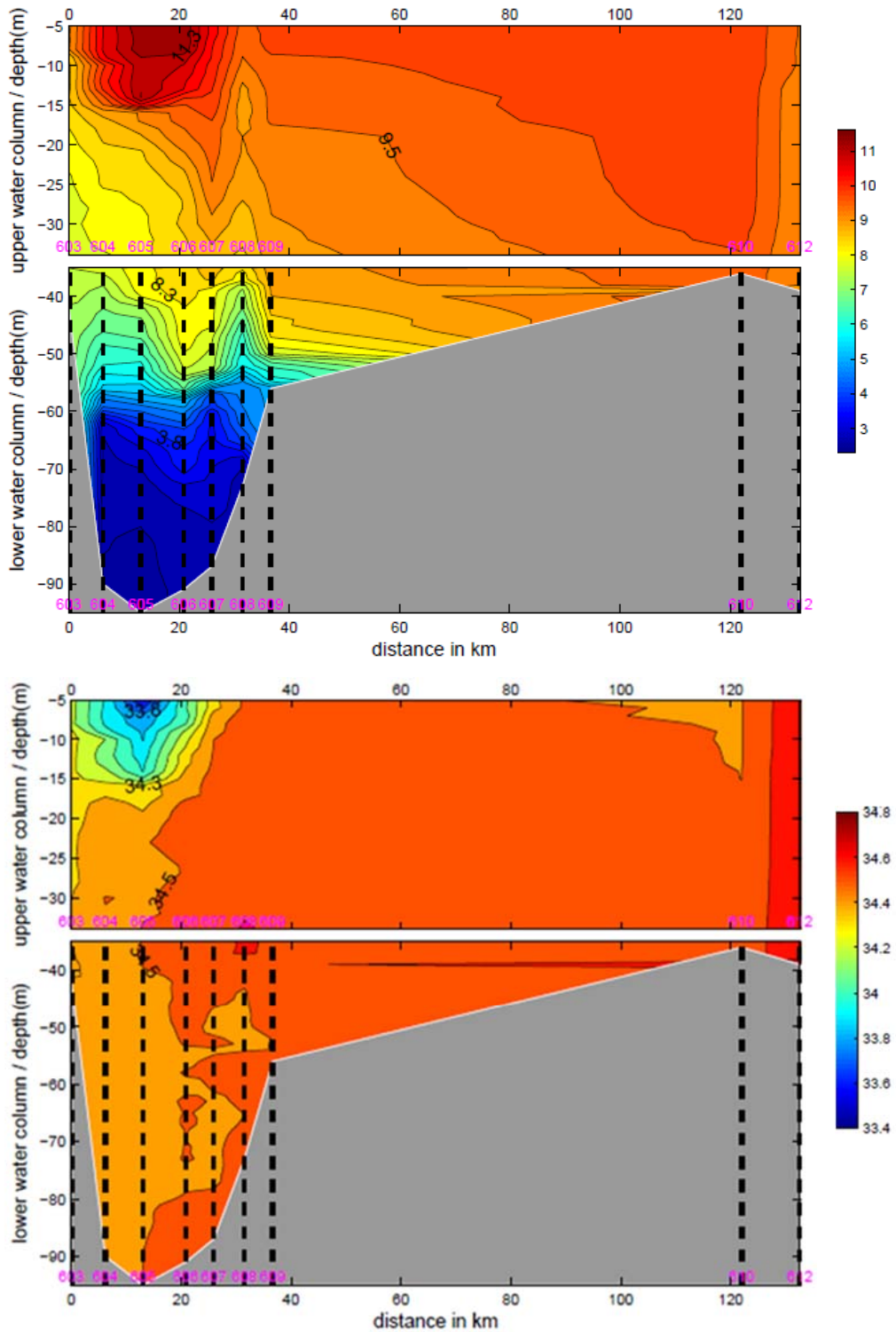
Fig. 5.12   Top: Temperature [°C] (top) and salinity (bottom) at Arnarfjörður separated in upper (< 35 m) and lower water column. Stations marked with black dashed lines and stations numbers.

Arnarfjörður is a shallow fjord system without glaciers. Therefore, we did not observe a fresh and cool surface layer (Fig. 5.12) as in the other two fjords. Compared to Kongsfjorden and Scoresby Sound, Arnarfjörður was warmer (up to 11°C) and the surface water (up to 40 m) was characterized by salinities around ~33. The deeper part of the fjord was filled with a water mass characterized by strongly layered decreasing temperature and stable salinity reaching a minimum temperature of ~3°C and a maximum salinity of 34.8 close to the bottom.

A surface salinity minimum and temperature maximum (stations 605 and 606) might be caused by the influence of an adjacent fjord.
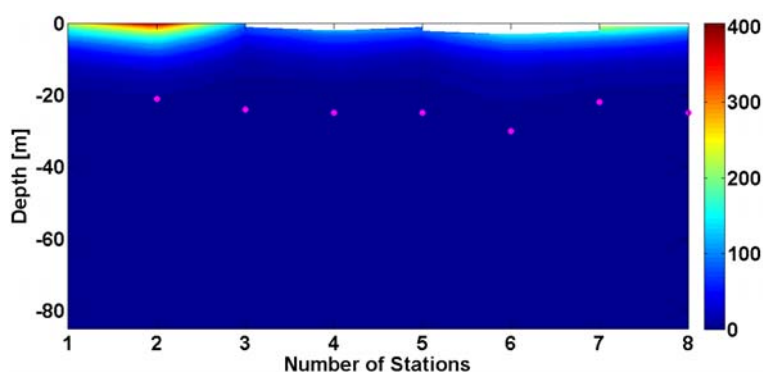
Fig. 5.13   Arnarfjörður (tip to mouth); Photosynthetically available radiation (PAR [µmol/m²s]) including 1% depth (magenta points) recorded by the free-falling light profiler.

The light field represented by PAR (Fig. 5.13) in Arnarfjörður was very homogenous during the two sampling days within the fjord. The 1% depth of PAR was similar at most stations and varied between 25 m and 30 m. Compared to Scoresby Sound, surface water light intensity in Arnarfjörður was much lower (PAR of up to 400 µmol/m²s).

5.3.3   Expected results

Fluorescence and oxygen data will be corrected with samples taken from the CTD water sampling rosette while salinity was already corrected on-board. ADCP data will be processed in more detail considering also tidal correction to get information about sources of water masses and the current within the fjord systems. A characterization of water masses within the three fjords will be conducted, based on temperature, salinity and other parameters such as CDOM. Hyperspectral radiometric data will be used to derive profiles of the downward diffuse attenuation coefficient and other apparent optical properties.

5.4   Phytoplankton mortality factors and impacts of glacier melting water
   (D. van de Waal)

5.4.1   Onboard sampling

At each station and depth, samples were taken for total bacteria and virus counts by means of flow cytometry. A 1 mL sample was fixed with glutaraldehyde to a final concentration of 0.5% (v/v), 30 min incubation at 4°C, flash-frozen in N_2 (l) and stored at -80°C.

At three stations in each fjord, i.e. 555, 557 and 559 (Kongsfjorden), 582, 590 and 593 (Scoresby Sound), and 603, 606 and 609 (Arnarfjörður), samples were taken for onboard incubations to assess microzooplankton grazing (Landry and Hassett, 1982). For each sample, water was filtered over a 200 μm mesh (fjord water), and half of the sample was subsequently gravity filtered over a 0.45 μm filter (grazer-free water). Dilutions of 100%, 70%, 40% and 20% fjord water were prepared in triplicate using the grazer-free water, with end volumes of 1L. Experiments were incubated at ambient temperatures (5°C, 3°C and 7°C, for Kongsfjorden, Scoresby Sound and Arnarfjörður, respectively) at an incident light intensity of 40±20 μmol photons m^{-2} s^{-1}. At the start of each incubation, samples were taken for cells counts with flow cytometry (3.5 mL, 0.5% formaldehyde + 1% hexamine, N_2 (l), stored at -80°C), Chl*a* (500 mL, N_2 (l), stored at -80°C), bacteria and virus counts (see above), and phytoplankton community (40 mL, >2% Lugol's iodine, stored at 4°C). After at least 24 h, samples were taken for cell counts with flow cytometry and Chl*a*. Mesozooplankton grazing was tested on stations 557 (Kongsfjorden) and 590 and 593 (Scoresby Sound), alongside the microzooplankton assays. To this end, one copepod was added to <200 μm filtered fjord water and incubated for >16 h. At the start and end of each incubation, samples were taken for cell counts with flow cytometry, and for Chl*a*.

To test the effect of glacier melt water on the plankton community, fjord water (station 590) was diluted with glacier water. Treatments included a control, 20% dilution, and 50% dilution. To correct for the dilution effect, 50% and 30% of 0.2 μm filtered fjord water was added to the control and 20% glacier water treatment, respectively. All incubations were performed in triplicate, and samples were taken at the start and after 5 days of incubation (at 3°C and incident light intensity of 40±20 μmol photons m^{-2} s^{-1}) for phytoplankton counts (L. Bach), bacteria and virus counts (D. van de Waal), Chl*a* concentration (van de Waal), phytoplankton community composition (van de Waal/Edvardsen), POC (C. Burau), dissolved inorganic nutrients (C. Burau), salinity (U. John), DOC (O. Lechtenfeld), microzooplankton numbers (M. Fernández-Méndez), ^{14}C primary production (M. Fernández-Méndez), ^{14}C bacterial production (L. McCallister), and metagenome (U. John).

5.4.2   First results

All samples will be analyzed after the cruise. Data is only available from the glacier melting water experiment, where direct cell counts were performed (flow cytometry, L. Bach). First results of the glacier melting water experiment demonstrate a clear shift in net phytoplankton growth rates, with distinct group specific responses (Fig. 5.14). All groups show an increased growth rate when fjord water was diluted with 20% glacier water, while with a further dilution down to 50%, growth rates either reduced (pico- and microplankton), remained unaltered (nanoplankton group II), or even increased (nanoplankton group I) as compared to the control.
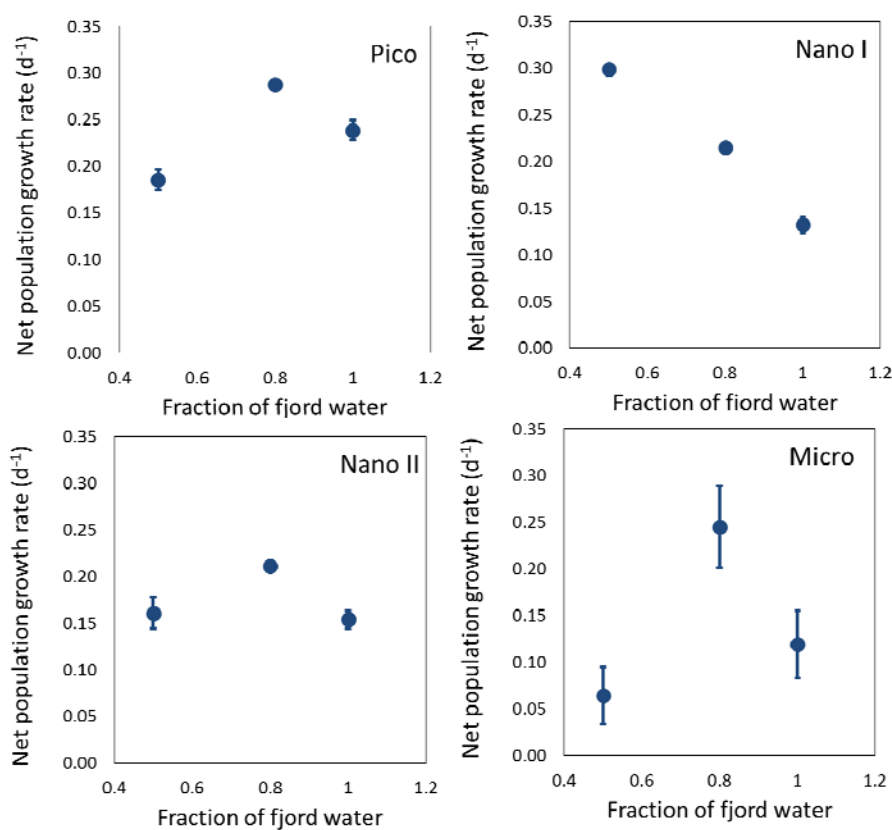
Fig. 5.14   Net population growth rates of different phytoplankton groups in relation to the dilution of fjord water with glacier water. Symbols indicate means±SD (n=3).

5.4.3   Expected results

Bacteria and virus counts will be performed after the cruise, in collaboration (NIOZ; C. Brusaard). These will describe gradients in abundances over the fjord gradients (from glacier to mouth), as well as depth. We predict a close association of bacteria to the abundance of primary producers, and of viruses with bacteria. To assess microzooplankton grazing, Chl*a* and phytoplankton cell counts will be performed after the cruise at NIOO. These data will allow calculating the relative impact of microzooplankton grazing on net phytoplankton growth,

which is expected to be higher just after the phytoplankton spring bloom as observed in Kongsfjorden and parts of Scoresby Sound.

All remaining analyses for the glacier melting water experiment will be performed by the respective groups upon return from the cruise. We expect a clear shift in phytoplankton community structure that may alter the release and composition of dissolved organic matter (DOM) in the water.

5.5   Abundance and distribution of phytoplankton functional groups
   (L. Bach)

5.5.1   Onboard sampling

Samples for phytoplankton functional type counts by means of flow cytometry were taken at almost all stations and depths. A 70 mL sample was tapped from the CTD bottles and directly processed with a Cytosense scanning and imaging flow cytometer (Cytobuoy) and an Accuri C6 flow cytometer (BD Biosciences). Population clusters were differentiated based on their fluorescence and scatter signal (Larsen et al., 2001;

Fig. 5.15). Images from the Cytosense were used to elucidate the taxonomic composition within larger (high forward scatter) population clusters.

The FL3-A (red fluorescence) signal from the Accuri C6 measurements was used to estimate the importance of phytoplankton groups relative to each other using equation 1:

$$X_{con} = \frac{X_{abundance} \times X_{FL3-A}}{All_{abundance} \times All_{FL3-A}} \qquad (1)$$

where X stands for one of the phytoplankton groups (Fig. 5.15, e.g. Picoeukaryotes), "con" refers to contribution of this particular group to the total FL3-A signal, abundance is the number of cells within gate X, FL3-A is the average red fluorescence of gate X, and "All" refers to a gate which includes all phytoplankton groups.
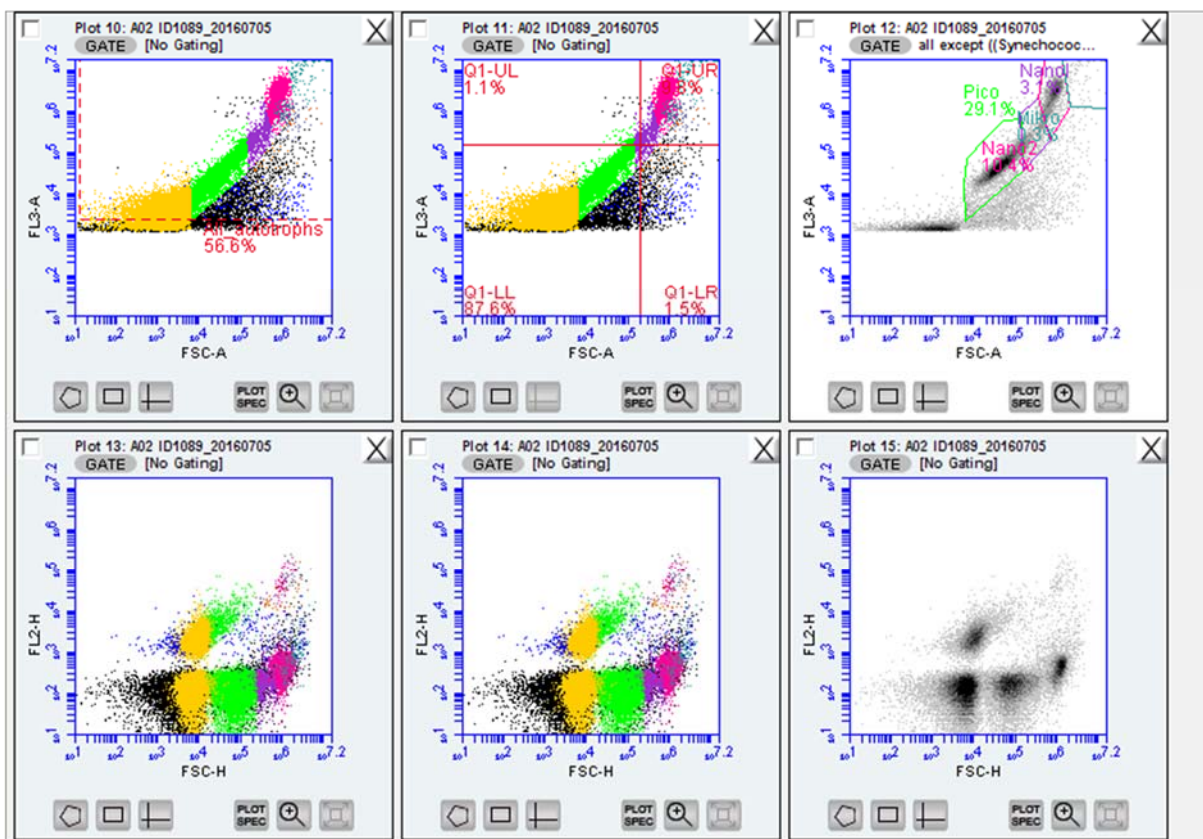
Fig. 5.15   Cytograms from the Accuri C6 flow cytometer counts. The gates in the top right subplot were the most important ones used during this cruise.

In Scoresby Sound, we set up an additional incubation experiment to test the effect of glacier melt water on the plankton community (see chapter 5.4).

5.5.2   First results

First results from the phytoplankton functional type abundance data is available from the transect in Kongsfjorden. Phytoplankon abundance (and biomass) was generally lower in close proximity to the glacier at the terminal end of the fjord (Fig. 5.16). Picoeukaryotes dominated the fluorescence red signal strength (a proxy for Chl*a* concentration) in the proximity of the glacier but then continuously decreased (Fig. 5.17). The marine influence became apparent with increasing distance to the glacier. *Phaeocystis spec.* started to become more abundant, as we identified based on Cytosense images () and microscopy. In general, there seemed to be a strong influence of North Atlantic water on the fjord system, which did not seem to be too isolated from the surrounding waters.
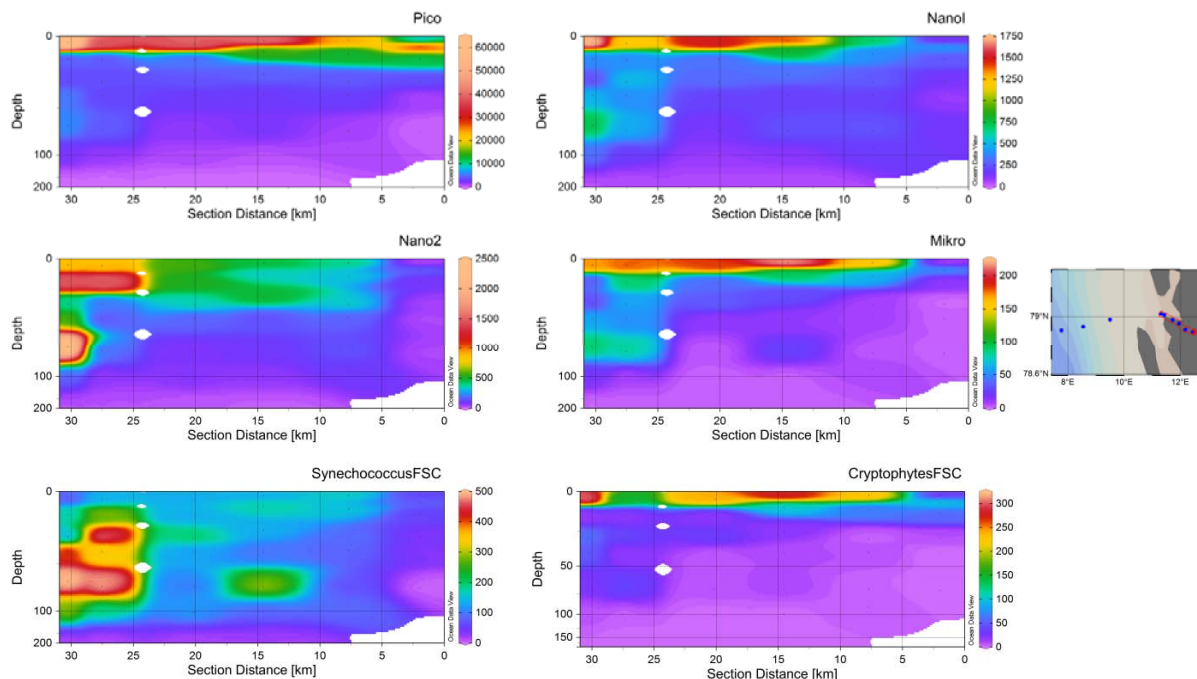
Fig. 5.16   Abundance of phytoplankton functional types determined with the Accuri C6 flow cytometer. Group names are listed on top of each subplot. The transect is illustrated on the right side. Contours show the abundance of cells per mL.
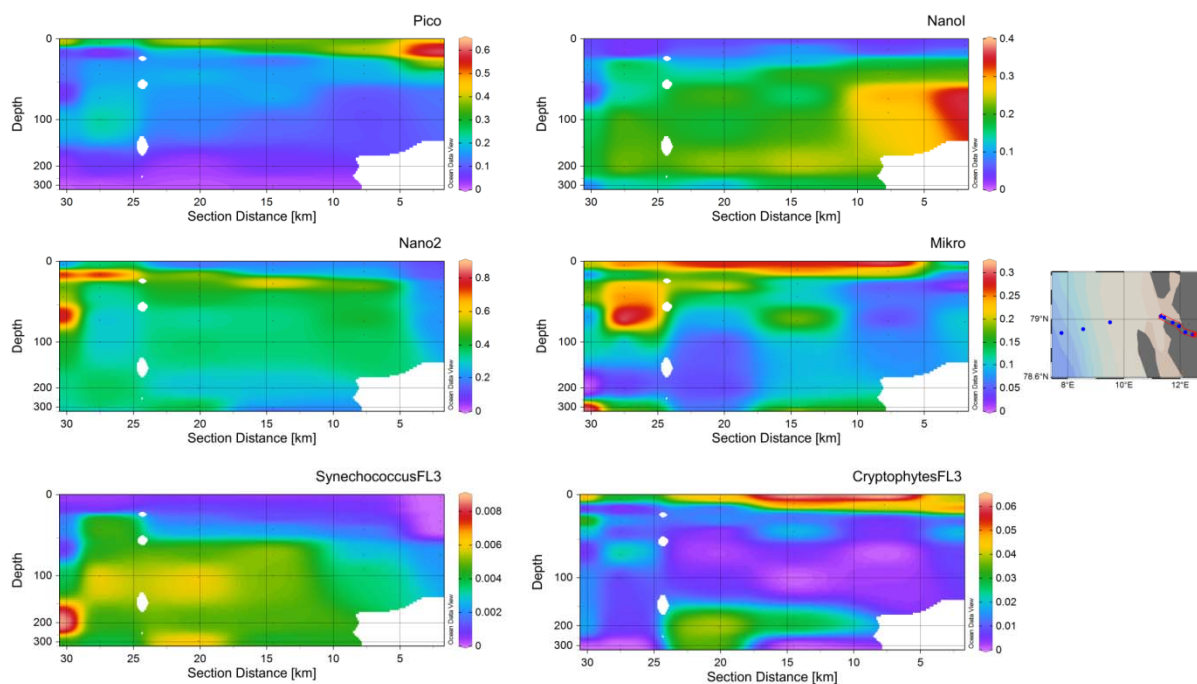
Fig. 5.17   Relative contribution (0 being 0% and 1 being 100%) to the total FL3-A signal measured with the Accuri C6 flow cytometer. Group names are listed on top of each subplot. The transect is illustrated on the right side. Contours show the relative contribution.
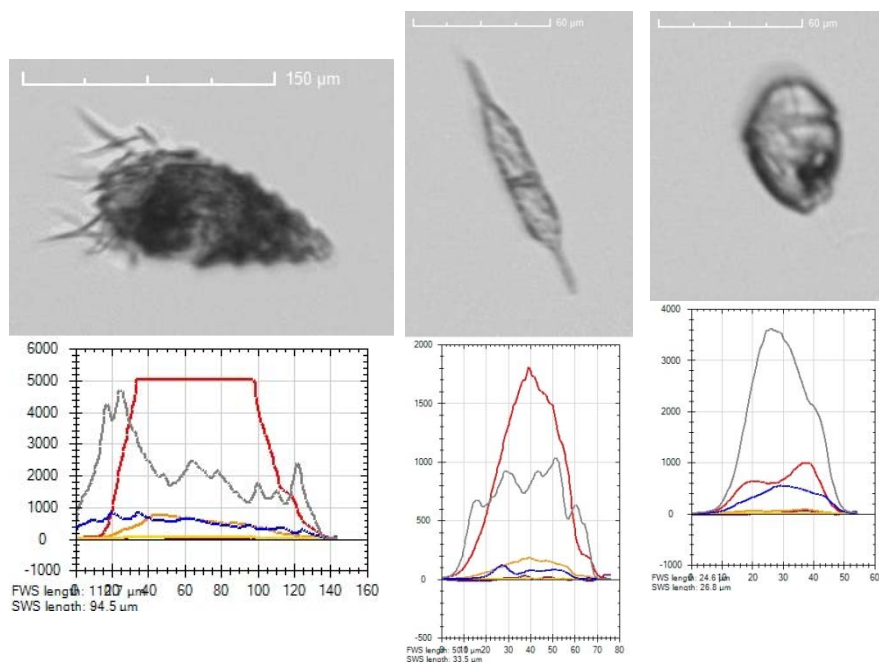
Fig. 5.18   Three example pictures from the analysis with the Cytosense imaging/scanning flow cytometer. The pictures of a Ciliate, a diatom, and a dinoflagellate are on top of their respective scans.

5.5.3   Expected results

A thorough evaluation of all flow cytometry data will follow this cruise. Similar data as the one shown in the contour plots for Kongsfjorden will then also be available for the Fram Strait transect (75°N), Scoresby Sound and Arnarfjörður (data analysis in close collaboration with U. John, S. Wohlrab, B. Edvardsen).

5.6   Marine Chemistry

(B.P. Koch, C. Burau, J. Geuer, O. Lechtenfeld,
P. Schmitt-Kopplin, M. Seifert, U. Wünsch)

5.6.1   Onboard sampling

Water samples were taken from each CTD cast for the standard depths surface, 15 m, chlorophyll maximum, 30 m, 40 m, 100 m and for deeper stations at 1000 m and bottom depth. The sampling scheme was adapted for gases, trace metals, DOC and POC.

Sampling for the noble-gases Helium/Neon was carried out in Kongsfjorden and in Scoresby Sound. Copper tubes were connected to the CTD and flushed to eliminate any air bubbles in the system. The tubes were then clamped off and stored at room temperature until analysis by mass spectrometry at the University of Bremen (O. Huhn).

Three depths of each station were sampled for dissolved oxygen (DO) in duplicates. Glass bottles were filled bubble free with seawater. The dissolved oxygen was then fixed by adding manganese chloride and sodium hydroxide/sodium iodide. Before titration, sulphuric acid was added to the sample, which was then titrated with thiosulfate. DO data will be used for post-cruise recalibration of the CTD oxygen sensor.

In Kongsfjorden, each depth of each station was sampled for dissolved inorganic carbon/total alkalinity. In Scoresby Sound, three depths per station were sampled. Glass vials were filled with seawater bubble free. Then, 1 mL of mercury chloride was added to the samples. Samples were sealed and stored at 4°C. Samples will be analysed by standard methods and used to evaluate the inorganic carbon system of each water mass.

Within each Fjord, trace element samples were taken at all stations and depths, avoiding the exposition to ambient air. After sampling, the volume was reduced to 50 mL and double distilled hydrochloric acid (36%) was added to acidify the samples to pH 1.8. The samples were stored at room temperature and will be analysed in the home-lab for total trace metal content.

Unfiltered water for nutrient analyses (nitrate, nitrite, ammonium, phosphate and silicate) was collected in 50 mL HDPE bottles directly from the CTD at every standard depth (total of 370 samples). Samples were immediately frozen at -20°C and will be analysed at AWI using standard procedures and a flow-injection analyser.

At each station, samples for the determination of oxygen isotopes ($\delta^{18}O$) were taken from the upper layer of the water column (upper 100 m, 230 samples total). Water was sampled into glass vials bubble-free. The vials were sealed with a mixture of melted bee wax and paraffin (50/50) and stored at 4°C.

At each standard depth, 1 L was taken from the CTD (370 samples) for the determination of DOC and total dissolved nitrogen (DON). The water was filtered with pre-combusted GF/F filters (~0.7 μm pore size) with low vacuum. 60 mL was filled into acid-cleaned HDPE-vials and stored at -20°C. For additional stations during the 75°N transect, DOC samples were obtained from a GF/F syringe filter after flushing the filter with excess sample. Samples will be

analysed in the home-lab for DOC and TDN with high-temperature catalytic oxidation. DON will be calculated as difference between TDN and the sum of inorganic nitrogen.

At each superstation, 1 L of seawater was filtered through GF/F for the analysis of (suspended) POC and nitrogen (PON). The filters were dried at 60°C for 48 h in aluminium foil and subsequently stored at -20°C.

Within the fjords, 236 water samples were solid-phase extracted for subsequent analyses of the DOM composition. After filtration with GFF filters (0.7 µm pore size) 500 mL of seawater was acidified to pH 2 with hydrochloric acid (30%). Solid-phase extraction cartridges (PPL, 200 mg) were conditioned with two fillings of methanol and acidified ultrapure water (pH 2, acidified with hydrochloric acid) before the sample was extracted. Another set of extraction combined three different adsorber materials sequentially (C8 followed by MAX followed by PPL) in 100 mg cartridges. 107 samples were extracted and produced 351 cartridges. The same conditioning procedure was applied and 500 mL water extracted systematically. After extraction, all cartridges were washed with two fillings of acidified ultrapure water. All cartridges were dried under a stream of nitrogen or by the application of vacuum. All cartridges will be eluted with methanol and analysed for organics and elements in the home institutes.

The optical properties of 333 CTD samples were analysed directly on board after filtration with GF/F filters (0.7 µm pore size). Both UV/Vis absorbance and fluorescence spectra were determined in the wavelength range of 240 – 600 nm according to established protocols (Stedmon and Nelson, 2015; Wunsch et al., 2018a; Wunsch et al., 2018b).

268 samples were taken from the CTD rosette and analysed for ammonium using an assay based on fluorescence of ortho-phthalaldehyde (Holmes et al., 1999).

An aerosol sampler was installed on the observation deck and which filtered, on average, 40 m³ in 24 h. Around 30 filters with 12, 24 and 36 h sampling intervals were collected using precombusted quartz filters (GFF). The collected filters were stored at -20°C and will be extracted in the home laboratory. To profile qualitatively the contribution of primary aerosol from seaburst, a bursting device was used in the lab on ship to produce bubble burst from waters of various salinity.

The ships seawater supply (6.5 m intake depth) was used to connect a pCO_2 sensor for continuous measurement of the CO_2 partial pressure in the surface water.

Iceberg debris was randomly selected and collected with the help of the ship's zodiac (1x Kongsfjorden, 2x Scoresby Sound). Ice was collected in double layered plastic bags and acid rinsed buckets. After return to the ship, the outer ice layers were removed via repetitive thaw-discard steps to remove potential contaminations. Melted glacier ice was sampled for trace metals, DOC, nutrients, CDOM/FDOM and bacterial production.

Glacier meltwater draining over land was also sampled (1x Kongsfjorden, 2x Scoresby Sound, 1x Arnarfjörður). Similar to the glacier meltwater, samples were split for analysis of trace metals, DOC, nutrients, CDOM/FDOM and bacterial production

Two experiments (Kongsfjorden and Scoresby Sound) were set up to test the biodegradability of various organic matter sources to the fjord systems. As endmembers, glacier meltwater, runoff, chlorophyll maximum depth water, and Atlantic water were chosen and incubated in the dark at 2-8°C (according to ambient surface water temperature). Regular subsamples for DOC, FDOM, bacterial counts and production were taken.

5.6.2 Onboard data

Optical properties of DOM

With a median fluorescence intensity of 0.012 Raman units at Excitation / Emission 350 / 450 nm and a median napherian absorbance of 0.15 m^{-1}, samples of MSM56 showed typical intensities of marine dissolved organic matter samples (Stedmon and Nelson, 2015). A preliminary model of the fluorescence data (methods as published in Murphy et al., 2013)) indicated the presence of six Parallel Factor analysis (PARAFAC) components (Fig. 5.19) that also matched those of multiple studies published in the OpenFluor database (Murphy et al., 2014). A more detailed analysis of covariance with molecular properties of the solid-phase extracted DOM will be used to investigate the chemical properties of DOM that track these fluorescent components.
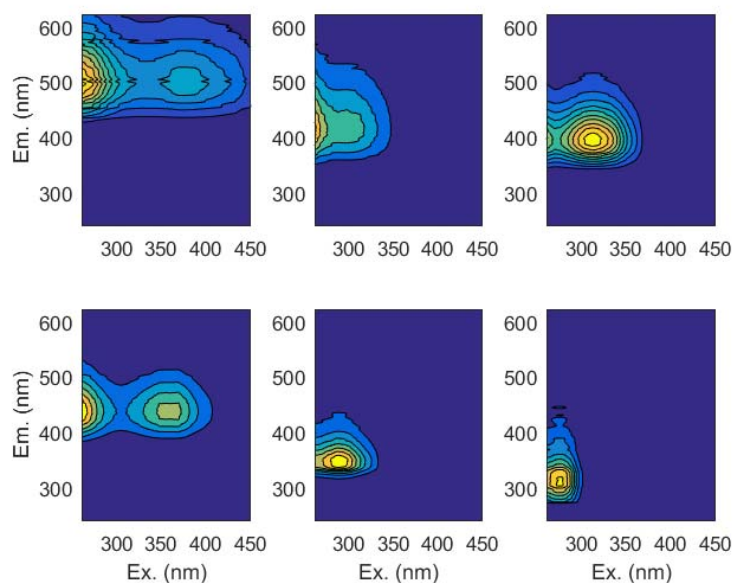
Fig. 5.19   Excitation and Emission properties of six preliminary Parallel Factor Analysis (PARAFAC) fluorescence components extracted from 329 samples measured onboard. Components are ordered according to their model contribution from top left to bottom right: C1 to C6.

5.6.3   First results

Ammonium

Preliminary results indicated low overall concentrations for ammonium in Scoresby Sound. Here, typical vertical profiles with a sharp maximum below the chlorophyll a maximum (maximum around 175 nmol L^{-1}) were observed, while all other samples indicated concentrations below the limit of detection. However, in Kongsfjorden and Arnarfjörður, ammonium concentrations were higher. Here, below the chlorophyll a maximum, ammonium concentrations exceeding 1 µmol L^{-1} were observed, while in ammonium was below the limit of detection in the surface layer.

5.6.4   Expected results

The oxygen measurements will help to calibrate the oxygen probe of the CTD. We are planning to identify glacial water input as well as water mass composition and dynamics by nutrient, $\delta^{18}O$ and Helium/Neon analysis.

We want to provide a high resolution profile of nutrients, DOM and CDOM and aim at characterizing the molecular differences in the extracts of different cartridges used. We also plan to evaluate the influence of glacial melt water and marine aerosols on the organic matter in the water column on a molecular level. Incubation experiments were performed to estimate the production and biodegradability of DOM. In connection to iron content in glacial ice (Bach), the content of other trace metals and presence of organic ligands that might enter the water column will be studied.

5.7   Biodiversity, Metatranscriptomics, and Metabolomics

(U. John, R. Amann, B. Edvardsen, M. Fernández-Méndez, N. Kühne, E. Nystedt, P. Schmitt-Kopplin, S. Wohlrab, J. Wulf)

Assessing the eukaryotic and prokaryotic biodiversity and link their composition, activity and metabolomics processes to the chemical and physical environment was one of the prime targets of the research cruise.

5.7.1   Onboard sampling

Sampling for molecular biodiversity (metabarcoding), metatranscriptomics and metametabolomics was achieved by three approaches (Fig. 5.20): 1) CTD/water-rosette; 2) plankton net (20 µm); 3) membrane pumping at discrete depth around Chl*a* maxima. Collected water samples were size fractionated into >200 µm, 200-100 µm, 100-20 µm with gravity power over filter towers and 20-3 µm and 3-0.2 µm size fractions in a series of tripode filtration units using a peristaltic pump collecting the plankton on polycarbonate filters.
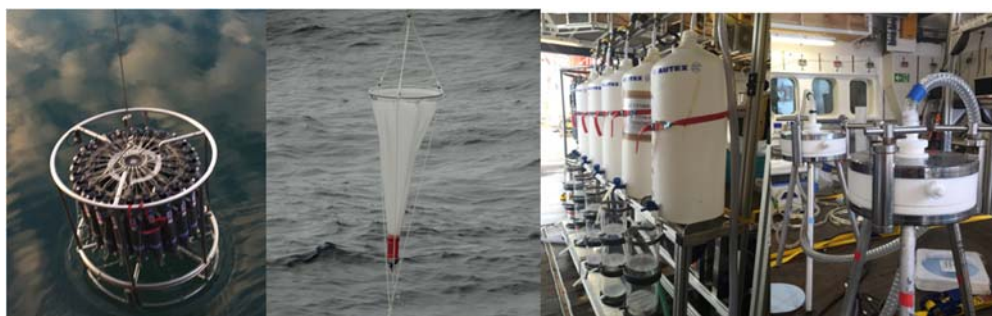
Fig. 5.20   Sampling and filter devices for molecular diversity and metatranscriptomics.

Plankton samples were divided for DNA and RNA extraction as well as for phycotoxin and metabolomics analysis. Polycarbonate filters were cut in four equal pieces, which were dedicated for DNA, RNA, metabolomics and one backup sample. Filters for metabolomics were immediately extracted with methanol and stored at -20°C for analysis in the home laboratory. 40 stations were sampled and 94 RNA samples were extracted and analyzed for quantity, purity and integrity. 208 DNA extractions and analyses were done onboard.

5.7.2   Expected results

Metabarcoding

PCR gene amplification of the V4 and V9 regions of the 18S rRNA and for the 3-0.2 µm size fraction also of 16S rRNA will be performed in the laboratory. Generated libraries will be Illumina MiSeq sequenced and the obtained data analyzed with the established bioinformatics pipelines at the AWI and MPI. Short sequences (reads) combined with metadata will be immediately published in public databases such as NCBI. Data will be analyzed with multifactorial statistics to elucidate the linkage of biodiversity and environmental parameters.

Metatranscriptomics

RNA samples of the three fjord systems will be used for cDNA library generation, which will be paired end sequenced at an in house (AWI) Illumina Nextseq platform. Obtained sequences of the corresponding libraries will be assembled into a reference metatranscriptome with the CLC Genomic Workbench software (www.clcbio.org). The assembled metatranscriptome will be functionally annotated (Trinnotate software environment) and assembled transcripts will be assigned to phylogenetic affiliation by BLAST search using a custom BLAST database constructed from reference transcriptomes. Finally, the reads obtained from each sequenced sample will be mapped against the reference metatranscriptome to obtain gene expression information. The results covering information about expression, identity and function of a respective contig within the metatranscriptome will be merged and evaluated with the R software environment implemented with the MANTA package (Marchetti et al., 2011).

Metabolomics

Metabolomics will be achieved on the methanol fractions in house (BGC/HMGU) using stepwise selected high resolution analytical techniques involving FT-ICR-MS, UPLC-QTOF/MS and NMR (P. Schmitt-Kopplin). The first method of choice will be ultrahigh resolution ICR-FT/MS in a direct injection mode. Exact masses will be annotated directly out of existing databased and unknown compounds linked with structural mass difference information in structural networks and metabolic pathways. Multivariate statistics (SIMCA/Umetrix) will evaluate the structure of the data as a function of the metadata collected during the cruise. The structure of relevant metabolites will be further investigated with tandem ICR-FT/MS, UPLC-QTOF/MS and NMR if needed. In a second step, this analyzed chemodiversity will be integrated with the biodiversity analysis. The cleaned metabolic signatures (knowns and unknowns) will be integrated with the metatranscriptome data acquired from the same samples using various R- and MatLab based programs developed in house (MassTRIX). The polyOmics datafusion will enable us to confine the various functional information obtained.

5.8   Taxonomic Diversity

 (B. Edvardsen, M. Fernández-Méndez, E. Nystedt)

5.8.1   Onboard sampling and data

Phytoplankton net samples were analyzed alive using inverted light microscopes (Fig. 5.21). A species list of microplankton diversity of most abundant taxa were generated for 30 stations. The diversity was documented by more than 500 micrographs (Fig. 5.22). For detailed plankton counting and examinations, the upper five CTD depths (0-30 m) were sampled for later analyses and preserved with glutardialdehyde/formaldehyde solution. Furthermore an integrated sample of the phytoplankton from the upper 30-40 m and larger than 20 μm was taken with a plankton net at 35 stations. In Kongsfjorden, two subsamples were preserved for further analysis, one with glutardialdehyde and formaldehyde and one with lugol. For the rest of the cruise only one sample was preserved with glutardialdehyde/formaldehyde solution.
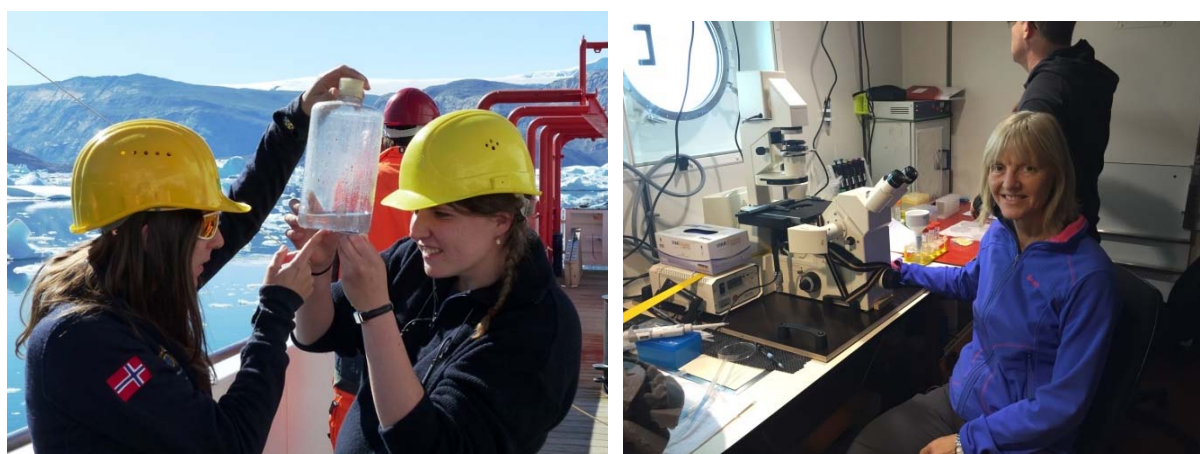
Fig. 5.21   Phytoplankton sample obtained from the hand net (left). Single cell isolation under the microscope (right).

Inner Kongsfjorden was dominated by heterotrohic and mixotrophic dinoflagellates (*Protoperidinium*, *Gymnodinium*, *Gyrodinium*), ciliates (*Parafavella, Ptychocylis*), zooplankton (incl. various larvae) and debris suggesting a post-bloom situation. The outer part was dominated by the haptophyte *Phaeocystis pouchetii* forming large colonies. The community on the 75°N transect was dominated by *Phaeocystis* in the East part and became more diverse in the mid and West part consisting of diatoms (e.g. *Rhizosolenia, Chaetoceros, Thalassiosira*), dinoflagellates (*Protoperidinium, Dinophysis)*, silicoflagellates (*Dictyocha*), and haptophytes (incl coccolithophores). In the inner part of Nordvestfjord of Scoresby Sound the dinoflagellate *Ceratium arcticum* and silicoflagellate *Octactis octonaria* were relatively abundant, the latter differed from the type variety. Algae associated to ice (*Fragilariopsis*) and other diatoms and dinoflagellates were also present. The mid-part showed a community with ciliates, zooplankton, dinoflagellates and diatoms suggesting a post-bloom situation. The inner

part of Arnarfjörður was characterized by zooplankton larvae, ciliates, heterotrophic and mixrotrophic dinoflagellates whereas the mid and outer part was strongly dominated by chain-forming small-celled diatoms such as *Skeletonema, Pseudo-nitzschia, Cylindrotheca, Dactyliosolen,* as well as dinoflagellates *(Dinophysis, Ceratium)* suggesting a summer situation with influence of silicate-rich water (e.g. land run-off).
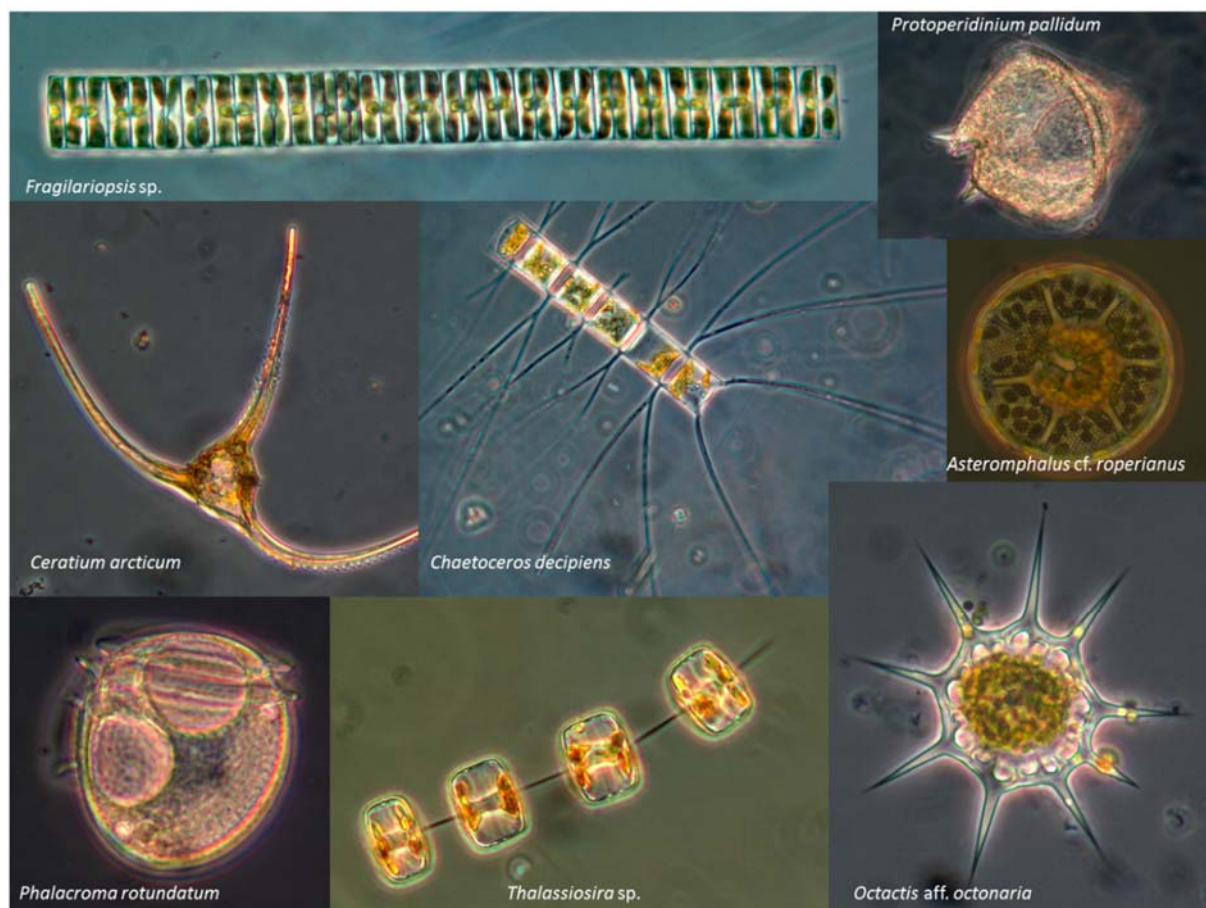
Fig. 5.22   Selected microphotographs from abundant microalgae (Photos: Edvardsen).

5.8.2   *Expected results*

Fixed samples will be analyzed and counted under the light microscope for quantitative data at IOPAS in Poland by Dr. Josef Viktor and his team. Furthermore, selected samples will be analyzed by electron microscopy at UiO for detailed taxonomic determinations.

5.9   Single cell isolation and PCR
 (B. Edvardsen, U. John)

To be able to link a DNA sequence of a marker gene to a morphospecies we need reference sequences. This is however missing for a large number of protists, such as of heterotrophic organisms, which are difficult to grow or to collect from remote places. Here we isolated 210 cells of microplankton protists from net samples by capillary pipetting under the light microscope. The morphology of each cell was documented by micrography. The cells were washed and transferred to a tube with PCR solutions and frozen. Some microalgal cells were picked to establish monoalgal cultures (see below). The taxonomic groups in focus were dinoflagellates, ciliates and diatoms, with additions of some silicoflagellates and haptophytes.

5.9.1   Onboard Data/First results

Gene amplification by PCR was performed with two primer sets for two molecular markers (18S and 28S rRNA genes). Amplicons were analysed with gel electrophoresis and gels inspected and documented under UV light on board.

Fifteen PCR reactions and corresponding gels were performed on board. Of 210 analysed cells about 70% was giving one or two bands on the gel, indicating successful amplification of one or both gene markers (Fig. 5.23).
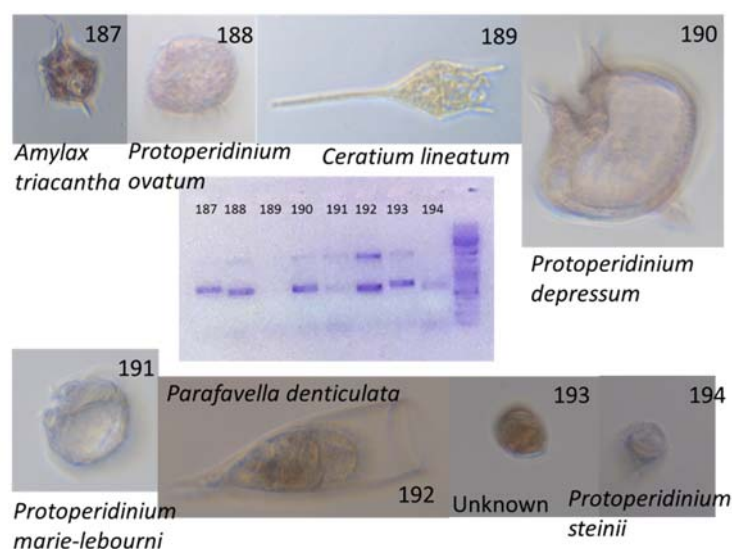
Fig. 5.23   Summary image of single cells isolated onboard. Light microscopic pictures were taking and names added where taxonomic identification was possible. The cells were further transferred to downstream PCR application. Numbers placed at the cell images corresponds to the lines at the 1% agarose gel image where the PCR amplicons were visualized. The upper band show the 18S rRNA and the lower band the D1D2 region of the 28S rRNA, on the right side the size marker was loaded.

5.9.2   *Expected results*

The remaining amplicons will be reamplified by nested PCR in the laboratory. The sequences will be edited, aligned and phylogenetic analyses performed to infer their relationships and taxonomic placements. We expect that we by this will improve the reference sequence database for Arctic microplankton and be able to more accurately than previous studies, reveal the protist community composition.

5.10   Bacterial Production
(S. McCallister)

5.10.1 Onboard sampling

Bacterial Production

Water samples were collected in each of the three fjords from 40 CTD stations. Bacterial production (BP) rates were derived from rates of ^{3}H-leucine incorporation measured on samples extending throughout the entire water column. The leucine assays followed a procedure modified from the protocol originally proposed by Smith and Azam, 1992. Briefly, triplicate 1.5 mL samples were incubated in the dark for 1-5h with ^{3}H-leucine (Perkin-Elmer; > 120 Ci/mmol, 25 nM final concentration) in 2.0 mL microcentrifuge tubes (Labcon SCT-200). Incubations were maintained within 2°C of the *in situ* temperature in refrigerated baths and terminated by the addition of 0.1 mL of 100% trichloroacetic acid (TCA). Samples were concentrated by centrifugation, rinsed with 5% TCA and 80% ethanol and air-dried overnight prior to radioassay by liquid scintillation counting in Ultima Gold cocktail (Perkin-Elmer). Blank values of TCA-killed samples were subtracted from the average of the triplicates.

Bacterial production was estimated as described by KIRCHMAN (1993), according to the equation BP = LI * 131.2 * (% Leu)$^{-1}$ * (C/protein) * ID, where BP is bacterial production, LI is the leucine incorporation rate (moles L^{-1} h^{-1}), 131.2 is the molecular weight of leucine, % Leu is the fraction of leucine in protein (0.073), C/protein is the ratio of cellular carbon to protein (0.86) and ID is the isotope dilution (2).

Influence of photochemistry on DOC bioavailabilty and molecular composition

To test the effect of UV exposure on DOC bioavailability and subsequent molecular composition, Scoresby Sound water collected from the chlorophyll maximum, and glacier melt water were filtered sequentially through a pre-baked 47 mm glass fiber filter (0.7μm) and a 0.2μm precleaned Supor Criticap to remove algae and bacteria. Sample water (100% fjord water, 100% glacial melt water and a 50:50 mixture of each) was transferred to 2.5L quartz tubes in duplicate and exposed to sunlight for 48 hours while temperature was maintained with a flow through water bath (fjord surface water, 8-10°C). Corresponding dark controls were covered with foil. All incubations were performed in duplicate. After sunlight exposure, samples were taken for DOC (Lechtenfeld), optical properties (Wünsch), and molecular composition (Lechtenfeld). Subsequently, 800 mL of each sample was distributed to 1 L glass bottles and inoculated with 20 mL of GF/F filtered water. Samples for bacterial production were taken at time 0, 1, 2 and 4 days while additional DOC and optical samples were collected at 6 days. Incubations will remain in cold container onboard (4°C), terminated upon return to AWI and sampled for final DOC and molecular composition (Lechtenfeld).

Additional samples

Samples for bacterial production were collected from Lechtenfeld's endmember incubations at various time points to assess the bioavailability of organic carbon sources. Bacterial production was determined for three treatments of dilution assay (Van de Waal). Samples for natural abundance radiocarbon were collected from sediment traps (van der Jagt), filtered through pre-baked 0.7 μm glass fiber filters and stored frozen.

5.10.2 Onboard data

All bacterial production samples were radioassayed onboard. Samples for radiocarbon analysis were transferred from AWI to VCU and processed and analyzed at Lawrence Livermore National Laboratory.

5.10.3 First results

Preliminary results indicate very low bacterial activity in glacial meltwaters suggesting a lack of bioavailable DOC. This is in contrast to recent studies that measured the rapid consumption of DOC in glaciers from Alaska suggesting significant regional differences in the importance of glacial derived DOC to the bacterial community. The exposure of glacial melt waters to natural sunlight did not enhance bacterial production; however, elevated production rates were measured in sunlight exposed fjord water (chl max) relative to dark controls.

5.10.4 Expected results

Further analyses will include calculating cell specific activity when bacterial abundance numbers are available. In addition, bacterial production only reflects the portion of carbon, which is allocated to bacterial growth, not the total amount of carbon consumed. The total flux of carbon through the microbial food web is equal to the sum of bacterial production and respiration (BR) and is termed bacterial carbon demand (BCD). Bacterial respiration will be computed from the formula $BR = 3.69 * BP^{0.58}$ (Robinson, 2008) and BCD estimated from the formula $BCD = BP + BR$. Integrated BP will be compared to integrated primary production in the photic zone. I anticipate the water column will be dominated by heterotrophic processes, which may exceed the in situ production of organic carbon by autotrophs.

5.11   Zooplankton and carbon export

   (C. Konrad, H. van der Jagt)

The sinking of marine snow aggregates (>0.5 mm) plays an important role in the ocean's carbon export fluxes. Marine snow aggregates are composed of phytoplankton cells, detritus, fecal pellets and inorganic mineral grains, and by settling the aggregates remove carbon from the surface ocean layer allowing the ocean to take up more atmospheric carbon dioxide. During this cruise, we investigated the particle fluxes in the water column and the role that zooplankton have on the attenuation of the carbon fluxes.

5.11.1 Onboard sampling

We captured particulate (organic) carbon flux with free-drifting sediment traps at seven stations: two in the Kongsfjorden, four in the Scoresby Sound and one in the Arnarfjörður (Fig. 5.24). We assessed the particle size-distribution and abundances in the water column with vertical particle camera profiles. The camera system was deployed 38 times. A Marine Snow Catcher collected *in situ* aggregates that were used on-board incubations and measurements. To study the role that zooplankton have on particle fluxes, we sampled zooplankton with multinet casts to estimate abundances and community composition. We used the four dominant zooplankton species for incubations with fresh aggregates in order to quantify the grazing impact from zooplankton on settling aggregates.

Drifting sediment traps

Fig. 5.24   Deployment of the drifting traps in the Scoresby Sound.

The drifting trap was composed of an array of sediment traps to sample the vertical carbon flux at different depths. During this cruise, we deployed the traps at 1) 50 m, 100 m and 200 m in the Kongsfjorden, 2) 100 m, 200 m and 400 m in the Scoresby Sound, and 3) 20 m and 70 m in the Arnarfjörður. One of the trap tubes contained a petri dish with a viscous gel at the bottom. The gel preserved the fragile structure and size of the captured sinking particles. These tubes contained three layers of different water densities, with in the middle layer 4% formaldehyde

added to fix and wash the samples *in-situ,* allowing for later DNA-staining and identification of particle-associated microbes (e.g. Flourescence In Situ Hybridisation and DAPI). The other tubes are used for biogeochemical fluxes such as total mass flux, the POC/PIC/PON and BSi flux (Seifert et al., 2019). Besides these measurements, samples were taken for genetics, microbial composition and ^{14}C-analysis.

Particle camera
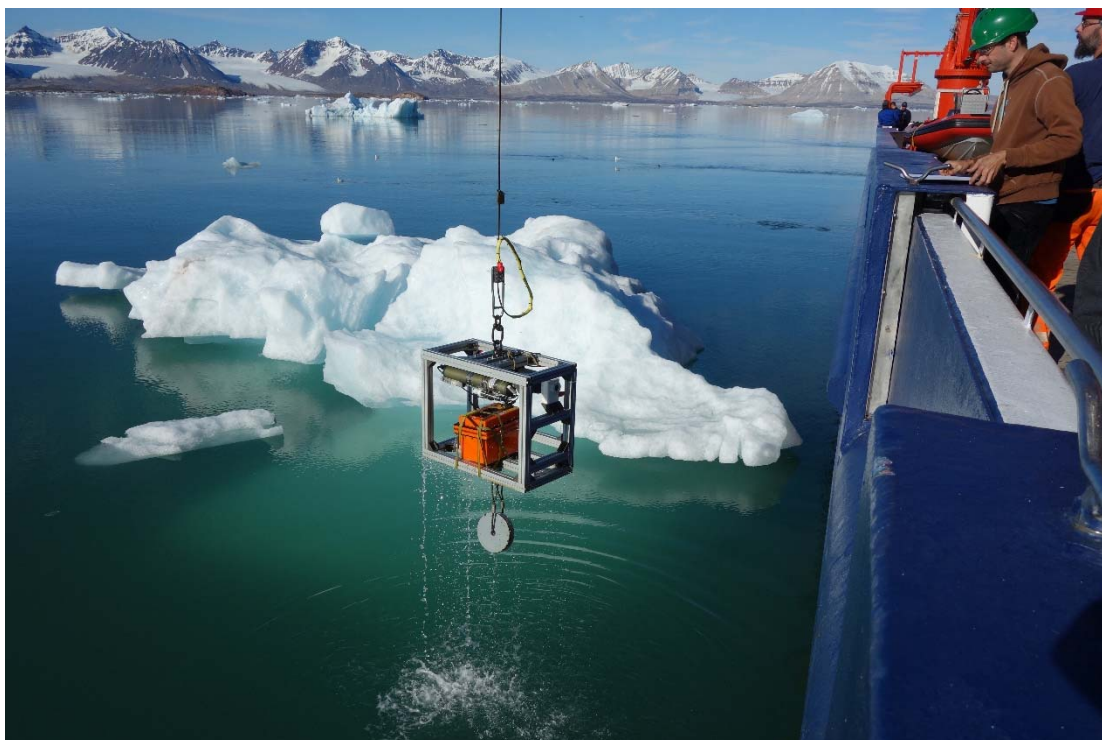
Fig. 5.25   The particle camera (ISC) deployed in Kongsfjorden.

The particle camera (ISC) was an infrared camera with backlight infrared illumination that can be used to investigate particle size-distribution and abundances in the water column (Fig. 5.25). It was equipped with a CTD that allowed us to relate the imaged particles to depth, salinity, temperature, turbidity, and fluorescence.

Zooplankton aggregate feeding

We investigated aggregate feeding by zooplankton. Although several studies have shown that zooplankton can feed on fecal pellets, there are a lack of direct observations of zooplankton grazing on marine snow. We expected this process to be important for carbon flux attenuation, since our previous measurements suggested that flux attenuation is larger than what can be explained by microbial degradation of marine snow.

We deployed a multinet (mesh size of 200μm) to collect live zooplankton for our incubations. In parallel to the multinet casts, we deployed the Marine Snow Catcher (MSC) to collect *in situ* formed aggregates (Fig. 5.26). We incubated four different zooplankton species

together with known concentrations of marine snow in gently rotating aquarium (roller tanks) to allow continuous sinking of the aggregates during the incubations. After the incubations we measured the loss of marine snow and the production of fecal pellets. Additionally, we made video recordings of each zooplankton species while offering settling marine snow in a 3D infrared camera setup. This provided detailed information about the feeding behavior of each of the four species.

Back in the home laboratory, we will calculate the potential effect that these species have on carbon flux attenuation. This will be done by relating the measured grazing rates by the four species on marine snow to the in situ abundance of both zooplankton and marine snow at different depths. By relating this to the observed vertical particle profiles and measured fluxes with the sediment traps, we can estimate the overall role of those species on the flux attenuation in the different fjords (Seifert et al., 2019).
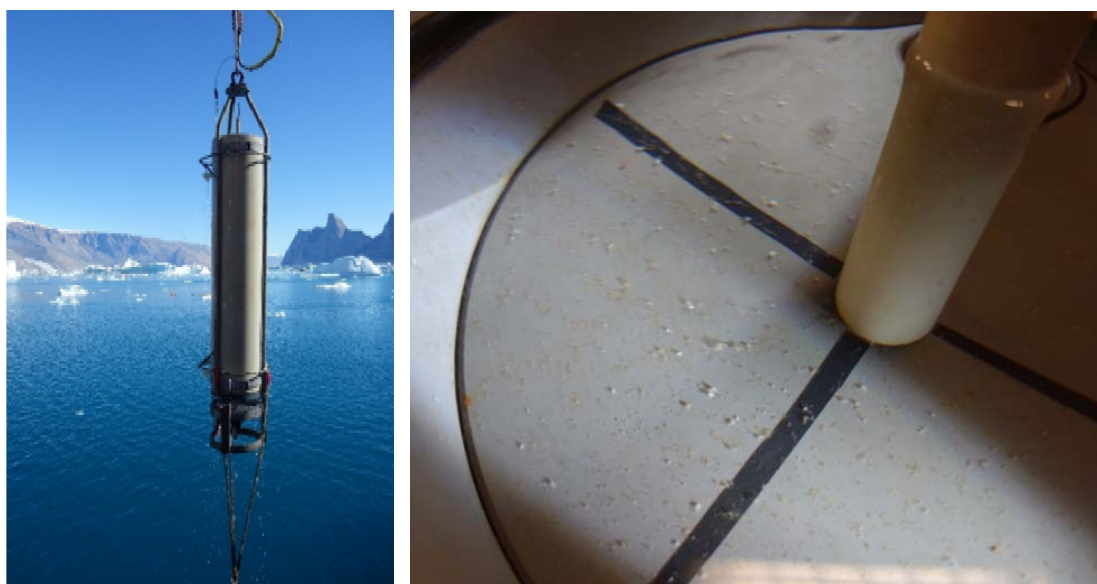
Fig. 5.26   The marine snow catcher deployed in the Scoresby Sound (left) and the respective collected aggregates (right).

5.11.2 First results

The sinking material collected with the sediment trap was significantly different between the three fjords. In the Kongsfjorden, the downward particle flux was dominated by fresh and degraded fecal pellets, whereas the particles collected in the Scoresby Sound were small phytoplankton aggregates and fecal pellets. The inner stations in both fjords were influenced by high concentrations of suspended inorganic minerals, presumably from glacial melting, that were partly incorporated into phytoplankton aggregates and fecal pellets. Especially in the Scoresby Sound the incorporation of the inorganic minerals had a strong 'ballasting' effect on the settling aggregates. We especially observed incorporation of inorganic minerals into fecal pellets at the outlet of the Nordvestfjord (592), which had high inorganic mineral concentration. The fecal pellets captured at the Nordvestfjord had a darker color and were small, suggesting

that the pellets were very dense as a result of inorganic mineral incorporation. At the outer station (572), where only little amounts of inorganic minerals were present, we observed fecal pellets with a light color, suggesting that the pellets mainly consisted of organic matter and had low densities (Fig. 5.27). The Arnarfjörður particle flux was dominated by large fecal pellets, and we managed to catch shrimps with both the gel trap and the multinet. We suspect that most of these fecal pellets are produced by shrimps that have escaped the local shrimp processing plant in Bíldudalur.
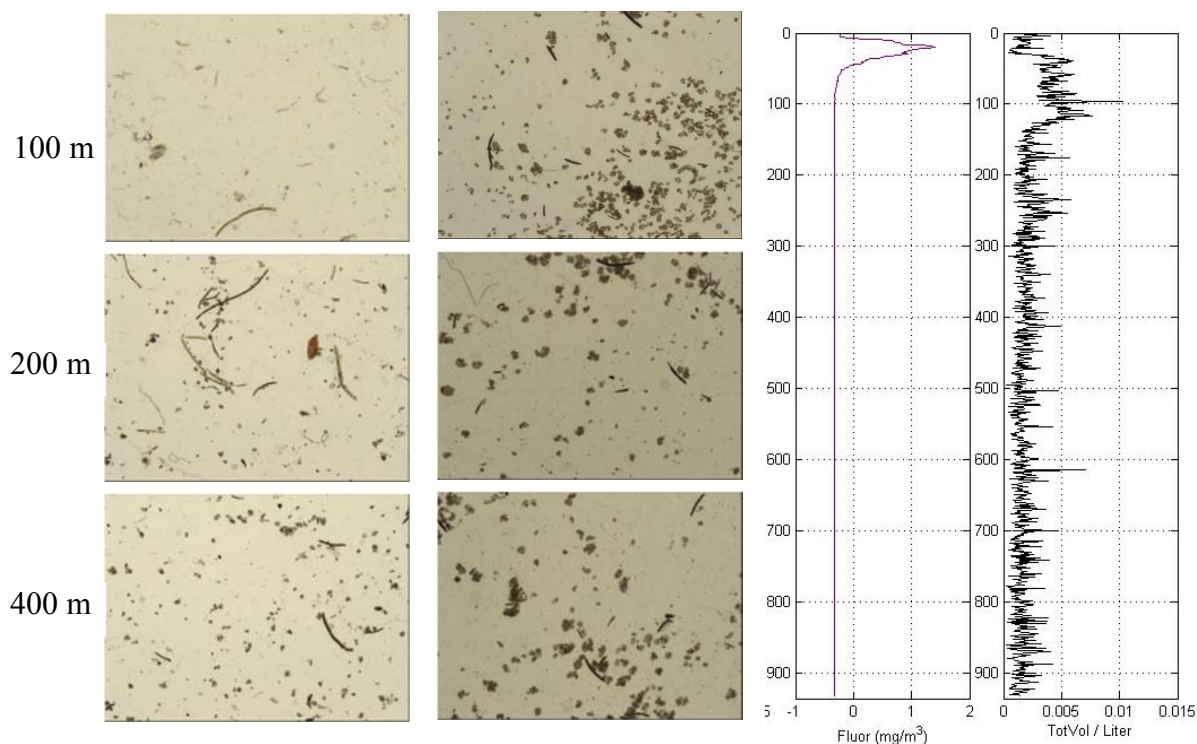
Fig. 5.27   Drifting trap gels containing sinking particles. Left: Station 572 (mouth of the Scoresby Sound), where fecal pellets dominated the particle flux. Middle: Station 592 (mouth of the Nordvestfjord), where the majority of the sinking material was small dense phytoplankton aggregates and fecal pellets containing lithogenic material. Right: Water column profile of station 592, showing fluorescence and total particle volume over depth.
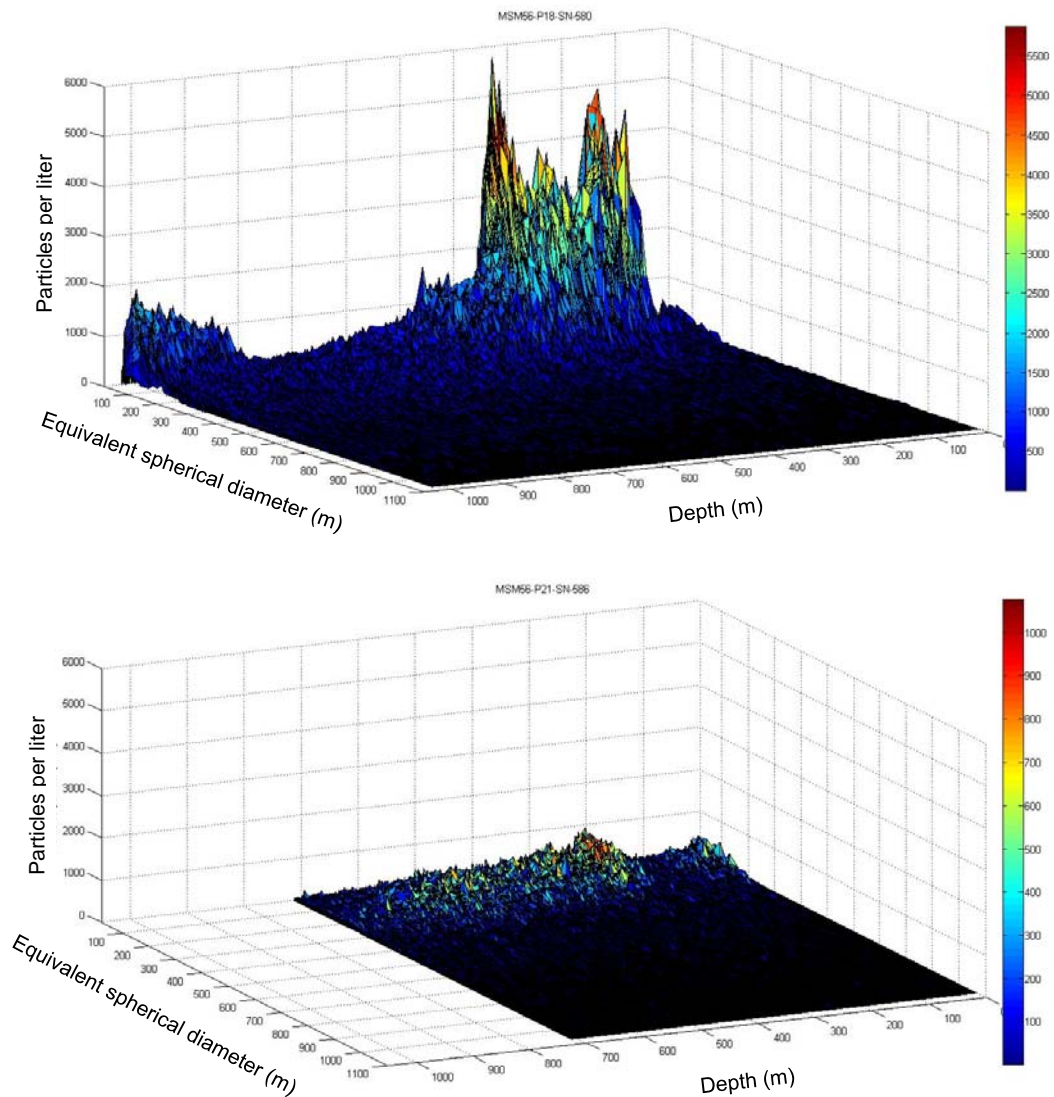
Fig. 5.28   Examples of particle camera profiles in Scoresby Sound. Upper: Station 580 (Nordvestfjord, where the Daugaard Jensen glacier terminates) with high changes of number of particles over the water column. Lower: Station 586 (further out in the Nordvestfjord) with lower particle abundances but with similar vertical distribution of particles.

First results of the measured particle profiles (Fig. 5.28) show quite high particle abundances through the water column in the inner parts of all three fjords (Kongsforden, Scoresby Sound and Arnarfjörður) compared to further out in the fjord systems and to open ocean (75°N transect).

First results of our zooplankton aggregate feeding showed that *Calanus glacialis*, *Calanus finmarchicus* and *Calanus hyperboreus* were feeding on sinking aggregates. However, compared to a previous a cruise where we investigated zooplankton aggregate feeding by *Pseudocalanus* sp. and *C. glacialis*, we only observed low feeding rates on aggregates by the copepods investigated during the present cruise. This could possibly suggest that aggregate feeding by copepods is seasonally dependent and likely determined by the availability of other food items in the water column.

5.11.3 Expected results

We will analyze the drifting trap samples to quantify mass, POC, PIC, PON and BSi particle fluxes. These values will thereafter be linked to the different particle types and sizes that were captured by the drifting traps in the different regions. Zooplankton multinet samples will be used to estimate zooplankton abundance of the studied species in the fjords, to enable linking zooplankton aggregate feeding experiments to particle fluxes.

Beside these measurements, we took samples in cooperation with R. Amann, U. John and S.L. McCallister to look into the bacterial community, the biodiversity and the age of sinking particles.

6. Station list RV MARIA S. MERIAN MSM56

Station MERIAN	Date* 2016	Time* [UTC]	Latitude* [°N]	Longitude*	Water Depth [m]	Remarks/Recovery Gear
MSM56_551	02.07.	09:02	79° 1.20'	11° 18.16' E	335	CTD, TRAP, MN, CAM, PLA, PUMP, SC, PRO, SD
MSM56_552	02.07.	17:26	78° 59.13'	11° 17.06' E	278	ADCP
MSM56_553	03.07.	04:03	78° 57.96'	12° 22.73' E	66	CTD, CAM, PLA, PRO, SD, ZOD
MSM56_554	03.07.	09:51	78° 55.80'	12° 22.93' E	58	CTD, CAM, PLA, PRO, SD
MSM56_555	03.07.	11:58	78° 53.80'	12° 26.42' E	80	CTD, MN, CAM, PLA, PUMP, SD
MSM56_556	03.07.	16:42	78° 54.76'	12° 10.82' E	96	CTD, MN, CAM, PLA, PUMP, PRO, SD
MSM56_557	03.07.	04:49	78° 57.25'	11° 57.15' E	342	CTD, TRAP, MN, CAM, PLA, PUMP, PRO, SD
MSM56_558	04.07.	10:35	78° 58.69'	11° 43.81' E	302	CTD, CAM, PLA, PUMP, PRO, SD
MSM56_559	04.07.	13:22	79° 00.68'	11° 25.65' E	346	CTD, CAM, PLA, PUMP, PRO, SD
MSM56_560	04.07.	16:36	79° 01.25'	11° 18.15' E	336	CTD, MN, CAM, PLA, PUMP, SC, PRO, SD
MSM56_561	05.07.	03:54	78° 58.77'	09° 29.82' E	225	CTD, CAM, PLA, PRO, SD
MSM56_562	05.07.	07:55	78° 55.96'	08° 32.71' E	300	CTD, CAM, PLA, PRO, SD
MSM56_563	05.07.	10:24	78° 54.39'	07° 45.98' E	1137	CTD, PLA, PRO, SD
MSM56_564	05.07.	13:45	79° 03.01'	07° 00.18' E	1327	CTD, CAM, PRO, SD
MSM56_565	06.07.	13:57	74° 59.99'	06° 59.93' E	1869	CTD, CAM, PLA, SD
MSM56_566	07.07.	06:01	74° 59.99'	02° 59.92' E	2499	CTD, PLA
MSM56_567	07.07.	14:02	75° 00.03'	00° 59.99' W	3527	CTD, CAM, SC, SD
MSM56_568	08.07.	05:59	75° 00.01'	05° 00.08' W	3558	CTD, PLA, PRO, SD
MSM56_569	08.07.	14:20	74° 59.99'	08° 59.98' W	3286	CTD, MN, CAM, SC, PRO, SD
MSM56_570	09.07.	06:21	74° 59.96'	12° 59.97' W	325	CTD, MN, CAM, PLA, SC, PRO, SD
MSM56_571	10.07.	05:50	71° 59.98'	20° 00.02' W	247	CTD, PLA, PRO, SD
MSM56_572	10.07.	16:20	70° 14.93'	21° 59.96' W	562	CTD, TRAP, MN, CAM, SC, PRO, SD
MSM56_573	10.07.	22:02	70° 24.02'	21° 57.36' W	145	ADCP
MSM56_574	11.07.	07:16	70° 00.00'	20° 00.08' W	280	CTD, PLA, PRO, SD
MSM56_575	11.07.	11:08	70° 05.96'	20° 59.98' W	437	CTD, PLA, PRO, SD
MSM56_576	12.07.	00:03	70° 55.38'	24° 58.69' W	360	CTD, SD
MSM56_577	12.07.	03:08	71° 20.80'	25° 19.20' W	1262	CTD, SD
MSM56_578	12.07.	07:12	71° 32.06'	26° 58.92' W	1225	CTD, SD
MSM56_579	12.07.	11:01	71° 46.59'	27° 40.33' W	1482	CTD, SD
MSM56_580	12.07.	17:59	71° 54.49'	28° 18.96' W	1083	CTD, CAM, PLA, PUMP, PRO, SD
MSM56_581	13.07.	06:22	71° 54.69'	28° 19.54' W	1084	ZOD
MSM56_582	13.07.	10:31	71° 55.94'	28° 07.23' W	534	CTD, TRAP, MN, CAM, PLA, PUMP, SC, PRO, SD, ZOD
MSM56_583	13.07.	19:45	71° 52.11'	27° 43.44' W	1353	CTD, SD
MSM56_584	14.07.	03:57	71° 47.04'	27° 40.24' W	1482	CTD, CAM, PLA, PUMP, PRO, SD
MSM56_585	14.07.	09:00	71° 44.36'	27° 21.25' W	464	CTD, SD
MSM56_586	14.07.	10:35	71° 40.10'	27° 16.58' W	1413	CTD, MN, CAM, PLA, PUMP, PRO, SD
MSM56_587	14.07.	18:40	71° 38.49'	27° 15.77' W	683	ADCP
MSM56_588	15.07.	06:02	71° 35.62'	27° 30.07' W	1057	CTD, PRO, SD
MSM56_589	15.07.	08:03	71° 37.19'	27° 40.32' W	255	ZOD
MSM56_590	15.07.	10:01	71° 31.99'	26° 57.72' W	1217	CTD, CAM, PLA, PUMP, PRO, SD
MSM56_591	15.07.	16:02	71° 29.43'	26° 28.96' W	877	ADCP
MSM56_592	15.07.	00:15	71° 30.83'	26° 28.24' W	1091	CTD, TRAP, MN, CAM, PLA, PUMP, SC, PRO, SD
MSM56_593	16.07.	06:01	71° 31.58'	26° 01.26' W	1220	CTD, PLA, PRO, SD
MSM56_594	16.07.	14:14	71° 26.89'	25° 32.85' W	1269	CTD, PRO, SD
MSM56_595	17.07.	03:08	71° 19.90'	25° 15.87' W	373	ADCP, CTD, TRAP, MN, CAM, PLA, PUMP, SC, PRO, SD
MSM56_596	18.07.	11:34	71° 20.64'	25° 18.91' W	1248	EM122
MSM56_597	18.07.	13:42	71° 15.12'	25° 18.22' W	837	ADCP
MSM56_598	18.07.	14:37	71° 13.84'	25° 09.55' W	502	CTD, CAM, PLA, PRO, SD
MSM56_599	19.07.	04:00	70° 50.50'	24° 57.61' W	357	CTD, CAM, PLA, PUMP, PRO, SD
MSM56_600	19.07.	09:07	70° 29.04'	24° 40.16' W	506	CTD
MSM56_601	19.07.	11:54	70° 17.94'	23° 41.84' W	489	CTD, MN, CAM, PLA, PUMP, PRO, SD, ZOD
MSM56_602	19.07.	17:03	70° 10.95'	22° 44.37' W	544	CTD
MSM56_603	21.07.	06:46	65° 46.39'	23° 12.59' W	51	CTD, MN, CAM, PLA, PUMP, PRO, SD, ZOD
MSM56_604	21.07.	09:01	65° 45.18'	23° 20.16' W	96	CTD, CAM, PLA, PRO, SD
MSM56_605	21.07.	11:02	65° 44.98'	23° 29.09' W	101	CTD, CAM, PLA, PUMP, PRO, SD
MSM56_606	21.07.	04:57	65° 44.27'	23° 38.60' W	97	CTD, TRAP, MN, CAM, PLA, PUMP, SC, PRO, SD
MSM56_607	22.07.	07:01	65° 46.18'	23° 44.96' W	93	CTD, CAM, PRO, SD
MSM56_608	22.07.	09:56	65° 47.96'	23° 50.85' W	73	CTD, CAM, PLA, PUMP, PRO, SD
MSM56_609	22.07.	12:23	65° 49.56'	23° 56.42' W	62	CTD, CAM, PRO, SD
MSM56_610	22.07.	16:00	65° 50.45'	24° 03.89' W	43	CTD, CAM, PLA, PUMP, PRO, SD
MSM56_611	23.07.	06:12	65° 50.57'	23° 53.27' W	67	ADCP
MSM56_612	23.07.	16:24	65° 53.97'	24° 15.02' W	45	CTD

Values for date, time, geographic coordinates and depth represent the first recording at each station.

Abbreviations

ADCP	Acoustic Doppler current profiler
CTD	CTD, rosette water sampler
TRAP	Drifting sediment trap
EM122	Deep-Sea multibeam echosounder
MN	Multiple net
CAM	Particle camera
PLA	Plankton net
PUMP	Water pump
SC	Snow catcher
PRO	Light profiler
SD	Secchi disc
ZOD	Zodiak

7. Data and sample storage and availability

A cruise summary report was compiled immediately after the cruise and submitted to the "Leitstelle" German Research Vessels at Hamburg University. The report is available through the online database PANGAEA (www.pangaea.de).

All raw and processed data are stored on central storage devices with regular backups at the corresponding institutes and are available upon request. Available data sets and responsible scientists are listed below.

Data	Repository and date of planned publication	Contact person	Affilia-tion	Contact
CTD	PANGAEA, published	Friedrichs, Zielinski	ICBM	anna.friedrichs@uol.de oliver.zielinski@uol.de
Bacterial community composition/ cell counts	PANGAEA, 2017	Amann	MPI	ramann@mpi-bremen.de
ADCP, Light profiler, Flow-through system	PANGAEA, 2017	Friedrichs, Zielinski	ICBM	anna.friedrichs@uol.de oliver.zielinski@uol.de
Molecular biodiversity	PANGAEA/CBI; 2017	John	AWI	Uwe.john@awi.de
Metatranscriptomics	NCBI; 2017	Wohlrab	AWI	Sylke.Wohlrab@awi.de
Species sequences	NCBI; 2017	John	AWI	Uwe.John@awi.de Bente.Edvardsen@ibv.uio.no
Bacterial production, Radiocarbon	PANGAEA, 2017	McCallister	VCU	slmccalliste@vcu.edu
Marine Chemistry	PANGAEA, 2017	Koch	AWI	Boris.Koch@awi.de

8. Acknowledgements

9. References

Fernandez-Mendez, M., Katlein, C., Rabe, B., Nicolaus, M., Peeken, I., Bakker, K., Flores, H., Boetius, A., 2015. Photosynthetic production in the central Arctic Ocean during the record sea-ice minimum in 2012. Biogeosciences 12, 3525-3549.

Holmes, R.M., Aminot, A., Kerouel, R., Hooker, B.A., Peterson, B.J., 1999. A simple and precise method for measuring ammonium in marine and freshwater ecosystems. Canadian Journal of Fisheries and Aquatic Sciences 56, 1801-1808.

Kirchman, D., 1993. Leucine incorporation as a measure of biomass production by heterotrophic bacteria, in: Kemp, P.F., Sherr, B.F., Sherr, E.B., Cole, J.J. (Eds.), Handbook of methods in Aquatic Microbial Ecology. Lewis Pub, pp. 509-512.

Landry, M.R., Hassett, R.P., 1982. Estimating the grazing impact of marine micro-zooplankton. Marine Biology. Marine Biology 67, 283-288.

Larsen, A., Castberg, T., Sandaa, R.A., Brussaard, C.P.D., Egge, J., Heldal, M., Paulino, A., Thyrhaug, R., Van Hannen, E.J., Bratbak, G., 2001. Population dynamics and diversity of phytoplankton, bacteria and viruses in a seawater enclosure. Marine Ecology and Progress Series 221, 47–57.

Marchetti, A., Schruth, D.M., Durkin, C.A., Parker, M.S., Kodner, R.B., Berthiaume, C.T., Morales, R., Allen, A.E., Armbrust, E.V., 2011. Comparative metatranscriptomics identifies molecular bases for the physiological responses of phytoplankton to varying iron availability. Proceedings of the National Academy of Sciences of the United States of America 109, 317-325.

Murphy, K.R., Stedmon, C.A., Graeber, D., Bro, R., 2013. Fluorescence spectroscopy and multi-way techniques. PARAFAC. Analytical Methods 5, 6557-6566.

Murphy, K.R., Stedmon, C.A., Wenig, P., Bro, R., 2014. OpenFluor- an online spectral library of auto-fluorescence by organic compounds in the environment. Analytical Methods 6, 658-661.

Platt, T., Harrison, W.G., Irwin, B., Horne, E.P., Gallegos, C.L., 1982. Photosynthesis and photoadaptation of marine phytoplankton in the Arctic. Deep-Sea Research Part a-Oceanographic Research Papers 29, 1159-1170.

Robinson, C., 2008. Heterotrophic bacterial respiration, in: Kirchmann, D.L. (Ed.), Microbial Ecology of the Oceans. Wiley, Hoboken, New Jersey, pp. 299-327.

Seifert, M., Hoppema, M., Burau, C., Elmer, C., Friedrichs, A., Geuer, J.K., John, U., Kanzow, T., Koch, B.P., Konrad, C., van der Jagt, H., Zielinski, O., Iversen, M.H., 2019. Influence of Glacial Meltwater on Summer Biogeochemical Cycles in Scoresby Sund, East Greenland. Frontiers in Marine Science 6.

Smith, D.C., Azam, F., 1992. A simple, economical method for measuring bacterial protein synthesis rates in seawater using 3H-leucine. Marine Microbial Food Web 6, 107–114.

Stedmon, C.A., Nelson, N.B., 2015. The optical properties of DOM in the Ocean, in: Hansell, D.A., Carlson, C.A. (Eds.), Biogeochemistry of Marine Dissolved Organic Matter. Elsevier, San Diego, pp. 481–508.

Wunsch, U.J., Acar, E., Koch, B.P., Murphy, K.R., Schmitt-Kopplin, P., Stedmon, C.A., 2018a. The Molecular Fingerprint of Fluorescent Natural Organic Matter Offers Insight into Biogeochemical Sources and Diagenetic State. Analytical Chemistry 90, 14188-14197.

Wunsch, U.J., Geuer, J.K., Lechtenfeld, O.J., Koch, B.P., Murphy, K.R., Stedmon, C.A., 2018b. Quantifying the impact of solid-phase extraction on chromophoric dissolved organic matter composition. Marine Chemistry 207, 33-41.